

Interactive comment on “Export fluxes in a naturally iron-fertilized area of the Southern Ocean: seasonal dynamics of particulate organic carbon export from a moored sediment trap (part 1).” by Rembauville et al.

Response to reviewer’s #3 comments on the revised submission.

We thank anonymous referee #3 for the careful reading of the revised manuscript. All of the Reviewer’s suggestions have been taken into account and the resulting modifications appear in a revised version of the manuscript following this answer. **R3-Cx : Referee comment, R3-Rx: authors response**

In the revised manuscript, the authors have significantly addressed many of the substantive issues raised in the three reviews. Most importantly they have withdrawn some of the emphasis on strong flux attenuation, since, as the referees pointed out, there is not sufficient evidence for this. They have also omitted some of the inappropriate comparisons. There is also now an appropriate emphasis on reporting the seasonal cycle as requested by the reviewers.

However, there is now inconsistency within the text on how the “flux attenuation” issue is dealt with and there remains text that does not sufficiently take account of the unanimous views of the referees and still puts an unjustified case for strong flux attenuation.

We thank Reviewer #3 for acknowledging the extensive modifications made to the manuscript. According to the Reviewer’s additional suggestions, we have modified further our discussion of strong flux attenuation.

STRONG FLUX ATTENUATION considerations

R3-C1: *In the paragraph of lines 452 – 462 commencing “The annual POC export of...” the first comparison is made with the KEOPS 1 Blain et al. (2007) estimate. It would be more relevant to first compare with the other KEOPS 2 results and move the KEOPS 1 comparison to later in this paragraph.*

R3-R1: We initially decided to start with a comparison of the annual estimates before comparing the short-term estimates of KEOPS2 and KEOPS1. However following the reviewer’s suggestion we now start with a comparison of the short term estimates before the annual estimate derived from KEOPS1.

R3-C2: *In lines 454 – 457 they state that: “On shorter time scales, the POC flux recorded in the moored sediment trap represents only a small fraction (3-8%) of the POC flux at the base of the mixed layer measured by the different methods during KEOPS 2 (Table 3).” In fact these other KEOPS 2 methods measure short sampling periods/ deployments and not the annual total. It would be more informative, here, to compare the individual techniques, for example the Jouandet et al (2014) values quoted in table 3 are actually very similar to the monthly values of the authors’ results given in table 1. It would much improve this section if the different methods were compared, in turn.*

R3-R2: Here we indeed compare spring and summer sediment trap fluxes with short-term estimates performed at 200 m from individual techniques in spring during KEOPS2 and summer during KEOPS1. We hope the new formulation of this paragraph is clearer. Moreover, the similarity between and the Jouandet et al. (2014) values at 350 m and the sediment trap values is discussed in the next paragraph lines 453-456: “*We note that low carbon export fluxes around 300 m have been previously reported on the Kerguelen plateau. In spring 2011, UVP derived estimates of POC export at 350 m equals 0.1 to 0.3 mmol m⁻² d⁻¹ (Table 3), a value close to our reported value of 0.15 mmol m⁻² d⁻¹.*” Although a discussion of each technique is out of the scope of this paper, we added a brief description of the techniques.

MS change lines 443-466: “*We first compared the sediment trap export fluxes with short-term estimates at 200 m in spring (KEOPS2) and summer (KEOPS1). The POC flux recorded in the moored sediment trap represents only a small fraction (3-8%) of the POC flux measured at the base of the winter mixed layer (200 m) by different approaches during the spring KEOPS2 cruise (Table 3). The same conclusion can be drawn when considering the comparison with different estimates made at the end of summer during KEOPS1. Moreover, the annual POC export of ~0.1 mol m⁻² y⁻¹ at 289 m (Table 1) represents only 2% of the indirect estimate of POC export (5.1 mol m⁻² y⁻¹) at the base of the WML (200 m) on the Kerguelen Plateau based on a seasonal DIC budget (Blain et al., 2007). The short term estimates are derived from a diverse range of methods. The ²³⁴Th proxy is based on the ²³⁴Th deficit relative to the ²³⁸U due to its adsorption on particles, and it subsequent conversion to carbon fluxes using measured POC:²³⁴Th ratios. (Coale and Bruland, 1985; Buesseler et al., 2006; Savoye et al., 2006). The UVP provides high resolution images of particles (>52 µm) and the particle size distribution is then converted to carbon fluxes using an empirical relationship (Guidi et al., 2008; Picheral et al., 2010). Drifting gel traps allows the collection, preservation and imaging of sinking particles (>71 µm) that are converted to carbon fluxes using empirical volume:carbon relationship (Ebersbach and Trull, 2008; Ebersbach et al., 2011; Laurenceau-Cornec et al., 2015). Finally, drifting sediment traps are conceptually similar to moored sediment traps but avoid most of the hydrodynamic biases associated with this technique (Buesseler et al., 2007a). The diversity of the methods and differences in depth where the POC flux was estimated render quantitative comparisons challenging. Nevertheless, POC fluxes measured at 289 m with the moored sediment trap are considerably lower than other estimates made at 200 m. This result indicates either extremely rapid attenuation of flux between 200 m and 300 m or significant sampling bias by the sediment trap.*”

R3-C3: Lines 475-476. “*the scenario of strong flux attenuation...*” is not well supported and this sentence should be deleted.

R3-R3: We reformulated this sentence and deleted “*the scenario of strong flux attenuation...*”

MS change lines 478 - 479: “*Our calculations are thus consistent with emerging observations of significant POC flux attenuation in the Southern Ocean.*”

R3-C4: In lines 493 – 495 they state “*Therefore the low fluxes observed likely result from a combination of collection bias (hydrodynamics and swimmers) and strong attenuation of the POC flux between the base of the WML and 300 m.*” This should be re-written to suggest that it is currently not possible to isolate a specific explanation for low flux values.

R3-R4: We reformulated this sentence.

MS change lines 498 - 501: “Therefore the low fluxes observed likely result from a combined effect of collection bias (hydrodynamics and swimmers) and attenuation between the base of the WML and 300 m. However, it is not possible with the current dataset to isolate a specific explanation for low flux values”

R3-C5: Lines 496-497: It is incorrect to say that the moored trap had a “Low collection efficiency” with reference to the ^{234}Th - derived flux estimates. Simply it should be stated that the methods yielded different results and this would be better discussed in the paragraph above in lines 452 – 462.

R3-R5: We deleted this sentence. Lines 487 - 501 are dedicated to the discussion of the lower fluxes usually recorded by sediment traps compared to ^{234}Th - derived fluxes.

R3-C6: Lines 497 – 499. “the numerous lines of evidence discussed above appear to converge on a scenario of rapid flux attenuation.”. This is not justified and should be deleted.

R3-R6: The paragraph lines 464 – 477 demonstrates from two independent measurements that attenuation coefficients (b-values) are high over the central Kerguelen Plateau and falls in the range of previously reported values for the Southern Ocean. However we followed the Reviewer’s suggestion and deleted this sentence.

R3-C7: Lines 656 – 661 in the “Conclusions” will also need to be re-written to downplay the “strong flux attenuation” emphasis.

R3-R7: We have rewritten the last sentences of this paragraph and deleted the “strong flux attenuation”.

MS change (Conclusions): “We report the seasonal dynamics of particulate organic carbon (POC) export under the winter mixed layer (289 m) of the naturally iron fertilized and productive central Kerguelen Plateau. Annual POC flux was remarkably low (98 mmol m^{-2}) and occurred primarily during two episodic (<14 days) flux events exported with a 1 month lag following two surface chlorophyll *a* peaks. Analysis of the hydrological conditions and a comparison with different estimates of POC fluxes in spring and summer at the same station suggests that the sediment trap was subject to possible hydrodynamic and biological biases leading to under collection of particle flux. Nevertheless the low POC export was close to other estimates of deep (>300 m) POC export at the same station and is consistent with high attenuation coefficients reported from other methods. We invoke heterotrophic microbial activity and mesozooplankton and mesopelagic fish activity as possible explanations for efficient carbon flux attenuation and/or transfer to higher trophic levels which results in a High Biomass, Low Export environment.”

R3-C8: Section 4.4 “Rapid flux attenuation over the Kerguelen Plateau” should be changed to reflect a less definitive case to e.g. “Evidence for flux attenuation...”

R3-R8: We changed the title of this section to “Evidence for significant flux attenuation over the Kerguelen Plateau”.

R3-C8: Finally, in the abstract (lines 40) “the large reduction” should be replaced with words to the effect of “a significant reduction” to achieve the appropriate nuance and line 31 “collection of only 15-30%...” should be deleted.

R3-R8: We changed “large reduction” to “significant reduction”. We also deleted the comparison with ^{234}Th fluxes in the abstract.

SECTION 4.3 Seasonal Dynamic of POC export.

R3-C9: Line 396 “The temporal lag...” An alternative explanation is that there is a later event from which the flux originates that was not expressed in surface chlorophyll (see below). This should be discussed with reference to the Rynearson et al (2013) study.

R3-R9: We already mentioned this potential explanation in the original version of the manuscript: lines 429 – 432: “The temporal lag of one month measured in the present study suggest either slow sinking rates ($<5 \text{ m d}^{-1}$) characteristic of single phytoplanktonic cells or faster sinking particles that do not originate from the peaks of surface production.” and lines 441 – 443: “The hypothesis of a mass production of nutrient-limited resting spores post-bloom with high settling rates explains the temporal patterns of export we observed (Rembauville et al., 2014)”.

To make this clearer we have modified that original sentence too:

MS change lines 406 – 409: “The temporal lag of one month measured in the present study suggest either slow sinking rates ($<5 \text{ m d}^{-1}$) characteristic of single phytoplanktonic cells or faster sinking particles that originate from sub-surface production peaks undetected by satellite.”

R3-C10: Line 427 “It is generally accepted that satellite detection depth is 20-50 m (Gordon and McCluney, 1975)...” The satellite detection depth is, in fact, not more than 20 m in these circumstances. See, for example, Fig. 3 of [Smith R.C. (1981) “Remote sensing and depth distribution of ocean chlorophyll” *Mar. Ecol. Prog. Ser.* 5, 359-361]. Since the minimum surface chorophyll indicated in Fig. 7 appears to exceed 0.2 micro-g/L, then 20 m would be a maximum. A phytoplankton biomass would therefore only have to be deeper than 20 m to be undetected by satellite. This is significant, since the resting spores collected in traps in the North Atlantic by Rynearson et al (2013) were not part of surface samples. This paper should also be cited here in a modified discussion.

R3-R10: We added the reference for the satellite detection depth and changed the corresponding sentence. The resting spore formation and the associated driving factors are fully discussed is the “Part 2” paper, including the Rynearson et al. (2013) reference. We choose not to discuss these points in detail in this “Part 1”. Furthermore, it is entirely possible in the Rynearson dataset that the *Chaetoceros* aff. *diadema* vegetative cells were not detected in the uppermost surface samples because resting spore formation and export had already occurred at the time of sampling, as in fact suggested by their dominance as settling particles several hundred metres deep. *Chaetoceros Hyalochaete* populations are certainly present at 10 m from station A3 on the Kerguelen plateau (Armand et al., 2008).

MS change lines 409 - 412: “It is generally accepted that satellite detection depth is 20-50 m (Gordon and McCluney, 1975), and can be less than 20 m when surface chlorophyll a exceed

$0.2 \mu\text{g L}^{-1}$ (Smith, 1981), which prevents the detection of deep phytoplanktonic biomass structures (Villareal et al., 2011)."

MINOR POINTS.

Line 208: delete "we" at end of line.

Change made.

Line 218: stop after "salts".

Change made.

Line 358: stop after (Table 2).

Change made.

Line 375: should be "Particle".

Change made.

Line 385: replace "rather than" with "in addition to".

Change made.

Line 387: "dynamics".

Change made.

Line 391: comma after "deployments".

Change made.

Line 397: should be "originate".

Change made.

Line 464: upper case Plateau; replace "equals" with "are".

Change made.

Line 466: replace "equals" with "is".

Change made.

Line 509: insert "the" after "documents".

Change made.

Lines 513, 514: "fish" not "fishes"

Change made.

REFERENCES.

Something seems to have gone wrong with Endnote: the Coale et al 2004a and 2004b are actually the same paper (Lines 767-784). Similarly: Lima et al 2014a,b Lines 948-951.

Change made.

Line 875: stray comma after date

Change made.

Line 918: Laurenceau seems now to be Laurenceau-Cornec.

Change made.

References

- Armand, L.K., Cornet-Barthaux, V., Mosseri, J., Quéguiner, B., 2008. Late summer diatom biomass and community structure on and around the naturally iron-fertilised Kerguelen Plateau in the Southern Ocean. *Deep Sea Res. Part II Top. Stud. Oceanogr.* 55, 653–676. doi:10.1016/j.dsr2.2007.12.031
- Blain, S., Quéguiner, B., Armand, L., Belviso, S., Bomblé, B., Bopp, L., Bowie, A., Brunet, C., Brussaard, C., Carlotti, F., Christaki, U., Corbière, A., Durand, I., Ebersbach, F., Fuda, J.-L., Garcia, N., Gerringa, L., Griffiths, B., Guiguer, C., Guillerm, C., Jacquet, S., Jeandel, C., Laan, P., Lefèvre, D., Lo Monaco, C., Malits, A., Mosseri, J., Obernosterer, I., Park, Y.-H., Picheral, M., Pondaven, P., Remenyi, T., Sandroni, V., Sarthou, G., Savoye, N., Scouarnec, L., Souhaut, M., Thuiller, D., Timmermans, K., Trull, T., Uitz, J., van Beek, P., Veldhuis, M., Vincent, D., Viollier, E., Vong, L., Wagener, T., 2007. Effect of natural iron fertilization on carbon sequestration in the Southern Ocean. *Nature* 446, 1070–1074. doi:10.1038/nature05700
- Buesseler, K.O., Antia, A.N., Chen, M., Fowler, S.W., Gardner, W.D., Gustafsson, Ö., Harada, K., Michaels, A.F., Rutgers v. d. Loeff, M., Sarin, M., Steinberg, D.K., Trull, T., 2007. An assessment of the use of sediment traps for estimating upper ocean particle fluxes. *J. Mar. Res.* 65, 345–416.
- Buesseler, K.O., Benitez-Nelson, C.R., Moran, S.B., Burd, A., Charette, M., Cochran, J.K., Coppola, L., Fisher, N.S., Fowler, S.W., Gardner, W.D., Guo, L.D., Gustafsson, Ö., Lamborg, C., Masque, P., Miquel, J.C., Passow, U., Santschi, P.H., Savoye, N., Stewart, G., Trull, T., 2006. An assessment of particulate organic carbon to thorium-234 ratios in the ocean and their impact on the application of 234Th as a POC flux proxy. *Mar. Chem., Future Applications of 234Th in Aquatic Ecosystems (FATE)* 100, 213–233. doi:10.1016/j.marchem.2005.10.013
- Coale, K.H., Bruland, K.W., 1985. ^{234}Th : ^{238}U Disequilibria Within the California Current. *Limnol. Oceanogr.* 30, 22–33.
- Ebersbach, F., Trull, T.W., 2008. Sinking particle properties from polyacrylamide gels during the KERguelen Ocean and Plateau compared Study (KEOPS): Zooplankton control of carbon export in an area of persistent natural iron inputs in the Southern Ocean. *Limnol. Oceanogr.* 53, 212–224. doi:10.4319/lo.2008.53.1.0212
- Ebersbach, F., Trull, T.W., Davies, D.M., Bray, S.G., 2011. Controls on mesopelagic particle fluxes in the Sub-Antarctic and Polar Frontal Zones in the Southern Ocean south of Australia in summer—Perspectives from free-drifting sediment traps. *Deep Sea Res. Part II Top. Stud. Oceanogr.* 58, 2260–2276. doi:10.1016/j.dsr2.2011.05.025
- Gordon, H.R., McCluney, W.R., 1975. Estimation of the depth of sunlight penetration in the sea for remote sensing. *Appl. Opt.* 14, 413–416.
- Guidi, L., Jackson, G.A., Stemmann, L., Miquel, J.C., Picheral, M., Gorsky, G., 2008. Relationship between particle size distribution and flux in the mesopelagic zone. *Deep Sea Res. Part Oceanogr. Res. Pap.* 55, 1364–1374. doi:10.1016/j.dsr.2008.05.014
- Jouandet, M.-P., Jackson, G.A., Carlotti, F., Picheral, M., Stemmann, L., Blain, S., 2014. Rapid formation of large aggregates during the spring bloom of Kerguelen Island: observations and model comparisons. *Biogeosciences* 11, 4393–4406. doi:10.5194/bg-11-4393-2014
- Laurenceau-Cornec, E.C., Trull, T.W., Davies, D.M., Bray, S.G., Doran, J., Planchon, F., Carlotti, F., Jouandet, M.-P., Cavagna, A.-J., Waite, A.M., Blain, S., 2015. The relative importance of phytoplankton aggregates and zooplankton fecal pellets to carbon export: insights from free-drifting sediment trap deployments in naturally iron-fertilised waters near the Kerguelen Plateau. *Biogeosciences* 12, 1007–1027. doi:10.5194/bg-12-1007-2015
- Picheral, M., Guidi, L., Stemmann, L., Karl, D.M., Iddaoud, G., Gorsky, G., 2010. The Underwater Vision Profiler 5: An advanced instrument for high spatial resolution studies of particle size spectra and zooplankton. *Limnol. Oceanogr. Methods* 8, 462–473. doi:10.4319/lom.2010.8.462
- Rembauville, M., Blain, S., Armand, L., Quéguiner, B., Salter, I., 2014. Export fluxes in a naturally fertilized area of the Southern Ocean, the Kerguelen Plateau: ecological vectors of carbon and biogenic silica to depth (Part 2). *Biogeosciences Discuss* 11, 17089–17150. doi:10.5194/bgd-11-17089-2014
- Rynearson, T.A., Richardson, K., Lampitt, R.S., Sieracki, M.E., Poulton, A.J., Lyngsgaard, M.M., Perry, M.J., 2013. Major contribution of diatom resting spores to vertical flux in the sub-polar North Atlantic. *Deep Sea Res. Part Oceanogr. Res. Pap.* 82, 60–71. doi:10.1016/j.dsr.2013.07.013
- Savoye, N., Benitez-Nelson, C., Burd, A.B., Cochran, J.K., Charette, M., Buesseler, K.O., Jackson, G.A., Roy-Barman, M., Schmidt, S., Elskens, M., 2006a. 234Th sorption and export models in the water column: A review. *Mar. Chem., Future Applications of 234Th in Aquatic Ecosystems (FATE)* 100, 234–249. doi:10.1016/j.marchem.2005.10.014
- Savoye, N., Benitez-Nelson, C., Burd, A.B., Cochran, J.K., Charette, M., Buesseler, K.O., Jackson, G.A., Roy-Barman, M., Schmidt, S., Elskens, M., 2006b. 234Th sorption and export models in the water column: A review. *Mar. Chem.* 100, 234–249. doi:10.1016/j.marchem.2005.10.014

- Smith, R.C., 1981. Remote sensing and depth distribution of ocean chlorophyll. *Mar. Ecol.-Prog. Ser.* 5, 359–361.
- Villareal, T.A., Adornato, L., Wilson, C., Schoenbaechler, C.A., 2011. Summer blooms of diatom-diazotroph assemblages and surface chlorophyll in the North Pacific gyre: A disconnect. *J. Geophys. Res. Oceans* 116, C03001. doi:10.1029/2010JC006268

1 **Export fluxes in a naturally iron-fertilized area of the Southern
2 Ocean: seasonal dynamics of particulate organic carbon export
3 from a moored sediment trap (part 1).**

4

5 M. Rembauville^{1,2}, I. Salter^{1,2,3}, N. Leblond^{4,5}, A. Gueneugues^{1,2} and S. Blain^{1,2}

6 ¹ Sorbonne Universités, UPMC Univ Paris 06, UMR 7621, LOMIC, Observatoire Océanologique, Banyuls-sur-Mer, France.

7

8 ² CNRS, UMR 7621, LOMIC, Observatoire Océanologique, Banyuls-sur-Mer, France.

9

10 ³ Alfred-Wegener-Institute for Polar and Marine research, Bremerhaven, Germany.

11

12 ⁴Sorbonne Universités, UPMC Univ Paris 06, LOV, UMR 7093, Observatoire Océanologique, Villefranche-sur-Mer, France

13

14 ⁵CNRS-INSU, LOV, UMR 7093, Observatoire Océanologique, Villefranche-sur-Mer, France

15

16

17 Correspondance to: M. Rembauville (rembauville@obs-banyuls.fr).

18

19

20 **Abstract**

21

22 A sediment trap moored in the naturally iron-fertilized Kerguelen plateau in the Southern
23 Ocean provided an annual record of particulate organic carbon and nitrogen fluxes at 289 m.

24 At the trap deployment depth current speeds were typically low ($\sim 10 \text{ cm s}^{-1}$) and primarily
25 tidal-driven (M2 tidal component). Although advection was weak, the sediment trap may have
26 been subject to hydrodynamical and biological (swimmer feeding on trap funnel) biases. **that**

27 ~~could explain the collection of only 15–30 % of the ^{234}Th derived flux~~. Particulate organic

28 carbon (POC) flux was generally low ($<0.5 \text{ mmol m}^{-2} \text{ d}^{-1}$) although two episodic export
29 events (<14 days) of $1.5 \text{ mmol m}^{-2} \text{ d}^{-1}$ were recorded. These increases in flux occurred with a

30 1-month time lag from peaks in surface chlorophyll and together accounted for approximately

31 40 % of the annual flux budget. The annual POC flux of $98.2 \pm 4.4 \text{ mmol m}^{-2} \text{ y}^{-1}$ was low

32 considering the shallow deployment depth, but comparable to independent estimates made at
33 similar depths (~300 m) over the plateau and to deep-ocean (>2 km) fluxes measured from
34 similarly productive iron-fertilized blooms. Although undertrapping cannot be excluded in
35 shallow moored sediment trap deployment, we hypothesize that grazing pressure, including
36 mesozooplankton and mesopelagic fishes, may be responsible for the ~~large~~ significant
37 reduction in POC flux beneath the base of the winter mixed layer. The importance of plankton
38 community structure in controlling the temporal variability of export fluxes is addressed in a
39 companion paper.

40

41 **1 Introduction**

42 The biological carbon pump is defined as the vertical transfer of biologically fixed
43 carbon in the ocean surface to the ocean interior (Volk and Hoffert, 1985). Global estimates of
44 Particulate Organic Carbon (POC) export cluster between 5 Pg C y^{-1} (Moore et al., 2004; Lutz
45 et al., 2007; Honjo et al., 2008; Henson et al., 2011; Lima et al., 2014) to 10 Pg C y^{-1} (Laws et
46 al., 2000; Schlitzer, 2004; Gehlen et al., 2006; Boyd and Trull, 2007; Dunne et al., 2007;
47 Laws et al., 2011). The physical transfer of dissolved inorganic carbon to the ocean interior
48 during subduction of water masses is two orders of magnitude higher (> 250 Pg C y^{-1} ,
49 Karleskind et al., 2011; Levy et al., 2013). The global ocean represents a net annual CO₂ sink
50 of 2.5 Pg C y^{-1} (Le Quéré et al., 2013), slowing down the increase of the atmospheric CO₂
51 concentration resulting from anthropogenic activity. Although the Southern Ocean (south of
52 44°S) plays a limited role in the net air-sea CO₂ flux (Lenton et al., 2013), it is a key
53 component of the global anthropogenic CO₂ sink representing one third the global oceanic
54 sink (~ 1 Pg C y^{-1}) while covering 20 % of its surface (Gruber et al., 2009). The solubility
55 pump is considered as the major component of this sink, whereas the biological carbon pump
56 is considered to be inefficient in the Southern Ocean and sensitive to iron supply.

57 Following “the iron hypothesis” in the nineties (Martin 1990), iron limitation of high
58 nutrient low chlorophyll (HNLC) areas, including the Southern Ocean, has been tested in
59 bottle experiments (de Baar et al., 1990) and through *in situ* artificial fertilization experiments
60 (de Baar et al., 2005; Boyd et al., 2007). Results from these experiments are numerous and
61 essentially highlight that iron limits macronutrient (N, P, Si) utilization (Boyd et al., 2005;
62 Hiscock and Millero, 2005) and primary production (Landry et al., 2000; Gall et al., 2001;
63 Coale et al., 2004) in these vast HNLC areas of the Southern Ocean. Due to a large
64 macronutrient repository the biological carbon pump in the Southern Ocean is considered to
65 be inefficient in its capacity to transfer atmospheric carbon to the ocean interior (Sarmiento

66 and Gruber, 2006). In the context of micronutrient limitation, sites enriched in iron by natural
67 processes have also been studied and include the Kerguelen islands (Blain et al., 2001, 2007),
68 the Crozet islands (Pollard et al., 2007), the Scotia Sea (Tarling et al., 2012), and the Drake
69 Passage (Measures et al., 2013). Enhanced primary producer biomass in association with
70 natural iron supply (Korb and Whitehouse, 2004; Seeyave et al., 2007; Lefèvre et al., 2008)
71 strongly support trace-metal limitation. Furthermore, indirect seasonal budgets constructed
72 from studies of naturally fertilized systems have been capable of demonstrating an increase in
73 the strength of the biological carbon pump (Blain et al., 2007; Pollard et al., 2009), although
74 strong discrepancies in carbon to iron sequestration efficiency exist between systems. To date,
75 direct measurements of POC export from naturally fertilized blooms in the Southern Ocean
76 are limited to the Crozet Plateau (Pollard et al., 2009; Salter et al., 2012). The HNLC
77 Southern Ocean represents a region where changes in the strength of the biological pump may
78 have played a role in the glacial-interglacial CO₂ cycles (Bopp et al., 2003; Kohfeld et al.,
79 2005) and have some significance to future anthropogenic CO₂ uptake (Sarmiento and Le
80 Quéré, 1996). In this context, additional studies that directly measure POC export from
81 naturally iron-fertilized blooms in the Southern Ocean are necessary.

82 POC export can be estimated at short timescales (days to weeks) using the ²³⁴Th proxy
83 (Coale and Bruland, 1985; Buesseler et al., 2006; Savoye et al., 2006), by optical imaging of
84 particles (e.g. Picheral et al., 2010) or by directly collecting particles into surface-tethered
85 sediment traps (e.g. Maiti et al., 2013 for a compilation in the Southern Ocean) or neutrally
86 buoyant sediment traps (e.g. Salter et al., 2007; Rynearson et al., 2013). Temporal variability
87 of flux in the Southern Ocean precludes extrapolation of discrete measurements to estimate
88 seasonal or annual carbon export. However seasonal export of POC can be derived from
89 biogeochemical budgets (Blain et al., 2007; Pollard et al., 2009) or be directly measured by
90 moored sediment traps (e.g. Salter et al., 2012). Biogeochemical budgets are capable of

91 integrating over large spatial and temporal scales but may incorporate certain assumptions and
92 lack information about underlying mechanisms. Direct measurement by sediment traps rely
93 on fewer assumptions but their performance is strongly related to prevailing hydrodynamic
94 conditions (Buesseler et al., 2007a), which can be particularly problematic in the surface
95 ocean. Measuring the hydrological conditions characterizing mooring deployments is
96 therefore crucial to address issues surrounding the efficiency of sediment trap collection.

97 The ecological processes responsible for carbon export remain poorly characterized
98 (Boyd and Trull, 2007). There is a strong requirement for quantitative analysis of the
99 biological components of export to elucidate patterns in carbon and biomineral fluxes to the
100 ocean interior (Francois et al., 2002; Salter et al., 2010; Henson et al., 2012; Le Moigne et al.,
101 2012; Lima et al., 2014). Long-term deployment of moored sediment traps in areas of
102 naturally iron fertilized production, where significant macro- and micro-nutrient gradients
103 seasonally structure plankton communities, can help to establish links between ecological
104 succession and carbon export. For example, sediment traps around the Crozet Plateau (Pollard
105 et al., 2009) identified the significance of *Eucampia antarctica* var. *antarctica* resting spores
106 for carbon transfer to the deep ocean, large empty diatom frustules for Si:C export
107 stoichiometry (Salter et al., 2012), and heterotrophic calcifiers for the carbonate counter pump
108 (Salter et al., 2014).

109 The increase in primary production resulting from natural fertilization might not
110 necessarily lead to significant increases in carbon export. The concept of “High Biomass, Low
111 Export” (HBLE) environments was first introduced in the Southern Ocean (Lam and Bishop,
112 2007). This concept is partly based on the idea that a strong grazer response to phytoplankton
113 biomass leads to major fragmentation and remineralization of particles in the twilight zone,
114 shallowing the remineralization horizon (Coale et al., 2004). In these environments, the
115 efficient utilization and reprocessing of exported carbon by zooplankton leads to fecal pellet

116 dominated, low POC fluxes (Ebersbach et al., 2011). A synthesis of short-term sediment trap
117 deployments, ^{234}Th estimates of upper ocean POC export and in situ primary production
118 measurements in the Southern Ocean by Maiti et al. (2013) has highlighted the inverse
119 relationship between primary production and export efficiency, verifying the HBLE status of
120 many productive areas in the Southern Ocean. The iron fertilized bloom above the Kerguelen
121 Plateau exhibits strong remineralization in the mixed layer compared to the mesopelagic,
122 (Jacquet et al., 2008) and high bacterial carbon demand (Obernosterer et al., 2008), features
123 consistent with a HBLE regime. Moreover, an inverse relationship between export efficiency
124 and zooplankton biomass in the Kerguelen Plateau region support the key role of grazers in
125 the HBLE scenario (Laurenceau-Cornec et al., 2015). Efficient grazer responses to
126 phytoplankton biomass following artificial iron fertilization of HNLC regions also
127 demonstrate increases in net community production that are not translated to an increase in
128 export fluxes (Lam and Bishop, 2007; Tsuda et al., 2007; Martin et al., 2013; Batten and
129 Gower, 2014).

130 POC flux attenuation with depth results from processes occurring in the euphotic layer
131 (setting the particle export efficiency, Henson et al., 2012) and processes occurring in the
132 twilight zone between the euphotic layer and \sim 1000 m (Buesseler and Boyd, 2009), setting
133 the transfer efficiency (Francois et al., 2002). These processes are mainly biologically-driven
134 (Boyd and Trull, 2007) and involve a large diversity of ecosystem components from bacteria
135 (Rivkin and Legendre, 2001; Giering et al., 2014), protozooplankton (Barbeau et al., 1996),
136 mesozooplankton (Dilling and Alldredge, 2000; Smetacek et al., 2004) and mesopelagic
137 fishes (Davison et al., 2013; Hudson et al., 2014). The net effect of these processes is
138 summarized in a power-law formulation of POC flux attenuation with depth proposed by
139 Martin et al. (1987) that is still commonly used in data and model applications. The b-
140 exponent in this formulation has been reported to range from 0.4 to 1.7 (Buesseler et al.,

141 2007b; Lampitt et al., 2008; Henson et al., 2012) in the global Ocean. Nevertheless, a change
142 in the upper mesopelagic community structure (Lam et al., 2011), and more precisely an
143 increasing contribution of mesozooplankton (Lam and Bishop, 2007; Ebersbach et al., 2011)
144 could lead to a shift toward higher POC flux attenuation with depth.

145 In this paper, we provide the first annual description of the POC and PON export
146 fluxes below the mixed layer within the naturally fertilized bloom of the Kerguelen Plateau
147 and we discuss the reliability of these measurements considering the hydrological and
148 biological context. A companion paper (Rembauville et al., 2014) addresses our final aim: to
149 identify the ecological vectors that explain the intensity and the stoichiometry of the fluxes.

150 **2 Material and Methods**

151 **2.1 Trap deployment and mooring design**

152 As part of the KEOPS2 multidisciplinary program, a mooring line was deployed at
153 station A3 ($50^{\circ}38.3\text{ S}$ – $72^{\circ}02.6\text{ E}$) in the Permanently Open Ocean Zone (POOZ), south of
154 the Polar Front (PF) (Fig. 1). The mooring line was instrumented with a Technicap PPS3
155 (0.125 m^2 collecting area, 4.75 aspect ratio) sediment trap and inclinometer (NKE S2IP) at a
156 depth of 289 m (seafloor depth 527 m) (Fig. 2). A conductivity-temperature-pressure (CTD)
157 sensor (Seabird SBE 37) and a current meter (Nortek Aquadopp) were placed on the mooring
158 line 30 m beneath the sediment trap (319 m). The sediment trap collection period started on
159 21 October 2011 until 7 September 2012. The sediment trap was composed of twelve rotating
160 sample cups (250 mL) filled with a 5 % formalin hypersaline solution buffered with sodium
161 tetraborate at $\text{pH} = 8$. Rotation of the carousel was programmed to sample short intervals (10-
162 14 days) between October and February, to optimize the temporal resolution of export from
163 the bloom, and long intervals (99 days) between February and September. All instruments had
164 a 1 hour recording interval. The current meter failed on the 7th April 2012.

165 **2.3 Surface chlorophyll data**

166 The MODIS AQUA level 3 (4 km grid resolution, 8 day averages) surface chlorophyll
167 *a* product was extracted from the NASA website (<http://oceancolor.gsfc.nasa.gov/>) for
168 sediment trap deployment period. An annual climatology of surface chlorophyll *a*
169 concentration, based on available satellite products (1997-2013), was calculated from the
170 multisatellite Globcolour product. The Globcolour level 3, (case 1 waters, 4.63 km resolution,
171 8 day averages) product merging Seawifs, MODIS and MERIS data with GSM merging
172 model (Maritorena and Siegel, 2005) was accessed via <http://www.globcolour.info>. Surface
173 chlorophyll *a* concentrations derived from Globcolour (climatology) and MODIS data

174 (deployment year) were averaged across a 100 km radius centered on the sediment trap
175 deployment location (Fig. 1).

176 **2.3 Time series analyses of hydrological parameters**

177 Fast Fourier Transform (FFT) analysis was performed on the annual time series data obtained
178 from the mooring, depth and potential density anomaly (σ_0) that were derived from the CTD
179 sensor. Significant peaks in the power spectrum were identified by comparison to red noise, a
180 theoretical signal in which the relative variance decreases with increasing frequency (Gilman
181 et al., 1963). The red noise signal was considered as a null hypothesis and its power spectrum
182 was scaled to the 99th percentile of χ^2 probability. Power peaks higher than 99 % red noise
183 values were considered to be statistically significant (Schulz and Mudelsee, 2002), enabling
184 the identification of periods of major variability in time series. In order to identify the water
185 masses surrounding the trap, temperature and salinity recorded by the mooring CTD were
186 placed in context to previous CTD casts conducted at A3 during KEOPS1 (39 profiles, 23
187 January 2005 - 13 February 2005) and KEOPS2 (12 profiles, from 15 - 17 November).

188 **2.4 Sediment trap material analyses**

189 Upon recovery of the sediment trap the pH of the supernatant was measured in every cup and
190 1 mL of 37 % formalin buffered with sodium tetraborate (pH=8) was added. After allowing
191 the particulate material to settle to the base of the sample cup (~24 hrs), 60 mL of supernatant
192 was removed with a syringe and stored separately. The samples were transported in the dark
193 at 4°C (JGOFS Sediment Trap Methods, 1994) and stored under identical conditions upon
194 arrival at the laboratory until further analysis. Nitrate, nitrite, ammonium and phosphate in the
195 supernatant were analysed colorimetrically (Aminot and Kerouel, 2007) to check for possible
196 leaching of dissolved inorganic nitrogen and phosphorus from the particulate phase.

197 Samples were first transferred to a petri dish and examined under stereomicroscope
198 (Leica MZ8, x10 to x50 magnification) to determine and isolate swimmers (i.e. organisms
199 that actively entered the cup). All swimmers were carefully sorted, cleaned (rinsed with
200 preservative solution), enumerated and removed from the cups for further taxonomic
201 identification. The classification of organisms as swimmers remains subjective and there is no
202 standardized protocol. We classified zooplankton organisms as swimmers if organic material
203 and preserved structures could be observed. Empty shells, exuvia (exoskeleton remains) and
204 organic debris were considered part of the passive flux. Sample preservation prevented the
205 identification of smaller swimmers (mainly copepods) but, where possible, zooplankton were
206 identified following Boltovskoy (1999).

207 Following the removal of swimmers, samples were quantitatively split into eight
208 aliquots using a Jencons peristaltic splitter. A splitting precision of 2.9 % (coefficient of
209 variation) was determined by weighing the particulate material obtained from each of four
210 1/8th aliquots (see below). Aliquots for chemical analyses were centrifuged (5 min at 3000
211 rpm) with the supernatant being withdrawn after this step and replaced by milliQ-grade water
212 to remove salts. ~~Milli-Q~~ rinses were compared with ammonium formate. Organic carbon
213 content was not statistically different although nitrogen concentrations were significantly
214 higher, consequently Milli-Q rinses were routinely performed. The rinsing step was repeated
215 three times. The remaining pellet was freeze-dried (SGD-SERAIL, 0.05-0.1 mbar, -30 °C to
216 30 °C, 48h run) and weighed three times (Sartorius MC 210 P balance, precision 10⁻⁴ g) to
217 calculate the total mass. The particulate material was ground to a fine powder and used for
218 measurements of particulate constituents.

219 For particulate organic carbon (POC) and particulate organic nitrogen (PON) analyses,
220 3 to 5 mg of the freeze-dried powder was weighed directly into pre-combusted (450°C, 24h)
221 silver cups. Samples were decarbonated by adding 20 µL of 2M analytical grade Hydrochloric

222 acid (Sigma-Aldrich). Acidification was repeated until no bubbles could be seen, ensuring all
223 particulate carbonate was dissolved (Salter et al., 2010). Samples were dried overnight at 50
224 °C. POC and PON were measured with a CHN analyzer (Perkin Elmer 2400 Series II
225 CHNS/O Elemental Analyzer) calibrated with glycine. Samples were analysed in triplicate
226 with an analytical precision of less than 0.7 %. Due to the small amount of particulate
227 material in sample cups #5 and #12, replicate analyses were not possible. Uncertainty
228 propagation for POC and PON flux was calculated as the quadratic sum of errors on mass flux
229 and POC/PON content in each sample. The annual flux (\pm standard deviation) was calculated
230 as the sum of the time-integrated flux.

231 **3. Results**

232 **3.1 Physical conditions around trap**

233 The sediment trap was deployed in the upper layers of Upper Circumpolar Deep Water
234 (UCDW), beneath seasonally mixed Winter Water (WW) (Fig. 2). The depth of the CTD
235 sensor varied between 318 m and 322 m (1 % and 99 % quantiles), with rare deepening to 328
236 m (Fig. 3a). Variations in tilt angle of the sediment trap were also low, mostly between 1 °
237 and 5 °, and occasionally reaching 13 ° (Fig. 3d). Current speed amplitude varied between 4
238 cm s^{-1} and 23 cm s^{-1} (1 % and 99 % quantiles) with a maximum value of 33 cm s^{-1} and a mean
239 value of 9 cm s^{-1} (Fig. 3e). Horizontal flow vectors were divided between northward and
240 southward components with strongest current speeds observed to flow northward (Fig. 3f and
241 3g).

242 The range in potential temperature and salinity was 1.85–2.23 °C and 34.12 – 34.26 (1
243 % - 99 % quantiles) (Fig. 3b and 3c). From July to September 2012, a mean increase of 0.2°C
244 in potential temperature was associated with a strong diminution of high frequency noise
245 suggesting a drift of the temperature sensor. Consequently these temperature data were

246 rejected from the time-series analysis. The potential temperature/salinity diagram is compared
247 to KEOPS1 and KEOPS2 CTD downcast at station A3 (Fig. 4). The CTD sensor recorded the
248 signature of the UCDW and no intrusion of overlying WW could be detected.

249 The power spectrum of vertical sediment trap displacements identified six significant
250 peaks corresponding to frequencies of 6.2 h, 8.2 h, 23.9 h, 25.7 h and 14 days (Fig 5a).
251 Concomitant peaks of depth, angle and current speed were also observed with a period of 14
252 days. However, spectral analysis of the potential density anomaly σ_0 revealed only one
253 significant major power peak corresponding to a frequency of 12.4 h (Fig. 5b). Isopycnal
254 displacements were driven by the unique tidal component (M2, 12.4h period) and trap
255 displacements resulted from a complex combination of multiple tidal components. The power
256 spectrum analysis suggested that a 40 hour window was relevant to filter out most of the short
257 term variability (black line in Fig 3a – 3e).

258 A pseudo-lagrangian trajectory was calculated by cumulating the instantaneous current
259 vectors (Fig 6). Over short time-scales (hours to day) the trajectory displays numerous tidal
260 ellipses. The flow direction is mainly to the South-East in October 2011 to December 2012
261 and North-East from December 2011 to April 2012. For the entire current meter record (6
262 months) the overall displacement followed a 120 km northeasterly, anticlockwise trajectory
263 with an integrated current speed of approximately 1 cm s^{-1} .

264 **3.2 Seasonality of surface chlorophyll *a* concentration above trap location**

265 The seasonal variations of surface chlorophyll *a* concentration for the sediment trap
266 deployment period differed significantly from the long-term climatology (Fig 7a). The bloom
267 started at the beginning of November 2011, ten days after the start of the sediment trap
268 deployment. Maximum surface chlorophyll *a* values of $2.5 \mu\text{g L}^{-1}$ occurred on the first week
269 of November and subsequently declined rapidly to $0.2 \mu\text{g L}^{-1}$ in late December 2011. A

270 second increase in surface chlorophyll *a* up to 1 $\mu\text{g L}^{-1}$ occurred in January 2012 and values
271 decreased to winter levels of 0.2 $\mu\text{g L}^{-1}$ in February 2012. A short-term increase of 0.8 $\mu\text{g L}^{-1}$
272 occurred in mid-April 2012.

273 **3.3 Swimmer abundances**

274 No swimmers were found in cups #3 and #5 (Table 2). Total swimmer numbers were highest
275 in winter (1544 individuals in cup #12). When normalized to cup opening time, swimmer
276 intrusion rates were highest between mid-December 2011 and mid-February 2012 (from 26 to
277 55 individuals d^{-1}) and lower than 20 individuals d^{-1} for the remainder of the year. Swimmers
278 were numerically dominated by copepods throughout the year, but elevated amphipod and
279 pteropod abundances were observed at the end of January and February 2012 (Table 2). There
280 was no significant correlation between mass flux, POC and PON fluxes and total swimmer
281 number or intrusion rate (Spearman's correlation test, $p > 0.01$). Copepods were essentially
282 small cyclopoid species. Amphipods were predominantly represented by the hyperidean
283 *Cyllopus magellanicus* and *Themisto gaudichaudii*. Pteropods were represented by *Clio*
284 *pyramidata*, *Limacina helicina* forma *antarctica* and *Limacina retroversa* subsp. *australis*.
285 Euphausiids were only represented by the genus *Thysanoessa*. One *Slapa thompsoni* salp
286 (aggregate form) was found in the last winter cup #12.

287 **3.4 Seasonal particulate organic carbon and nitrogen fluxes**

288 Particulate organic carbon flux ranged from 0.15 to 0.55 $\text{mmol m}^{-2} \text{d}^{-1}$ during the productive
289 period except during two short export events of 1.6 ± 0.04 and $1.5 \pm 0.04 \text{ mmol m}^{-2} \text{ d}^{-1}$
290 sampled in cups #4 (2 to 12 December 2011) and #9 (25 January to 8 February 2012),
291 respectively (Fig. 7b). The two flux events occurred with an approximate time lag of one
292 month compared to peaks in surface chlorophyll *a* values. A modest value of $0.27 \pm 0.01 \text{ mmol}$
293 $\text{m}^{-2} \text{ d}^{-1}$ was observed in autumn (cup #11, 22 February to 30 May 2012). The lowest POC flux

294 was measured during winter ($0.04 \text{ mmol m}^{-2} \text{ d}^{-1}$, cup #12, 31 May to 7 October). Assuming
295 that POC export was negligible from mid September to mid October, the annually integrated
296 POC flux was $98.2 \pm 4.4 \text{ mmol m}^{-2} \text{ y}^{-1}$ (Table 1). The two short (<14 days) export events
297 accounted for $16.2 \pm 0.5 \%$ (cup #4) and $21.0 \pm 0.6 \%$ (cup #9) of the annual carbon export out
298 of the mixed layer (Table 1). Mass percentage of organic carbon ranged from 3.3 % to 17.4 %
299 (Fig. 7b). Values were slightly higher in autumn and winter (respectively $13.1 \pm 0.2 \%$ and
300 $11 \pm 2.1 \%$ in cups #11 and #12) than in the summer, with the exception of cup #5 where the
301 highest value of 17.4 % was observed. PON fluxes followed the same seasonal patterns as
302 POC. This resulted in a relatively stable POC:PON ratio that varied between 6.1 to 7.4, except
303 in the autumn cup #11 where it exceeded 8.1 (Table 1).

304 **4 Discussion**

305 **4.1 Physical conditions of trap deployment**

306 Moored sediment traps can be subject to hydrodynamic biases that affect the accuracy of
307 particle collection (Buesseler et al., 2007a). The aspect ratio, tilt and horizontal flow regimes
308 are important considerations when assessing sediment trap performance. Specifically, the line
309 angle and aspect ratio of cylindrical traps can result in oversampling (Hawley, 1988).
310 Horizontal current velocities of 12 cm s^{-1} are often invoked as a critical threshold over which
311 particles are no longer quantitatively sampled (Baker et al., 1988). During the sediment trap
312 deployment period we observed generally low current speeds (mean $< 10 \text{ cm s}^{-1}$) with 75% of
313 the recorded data lower than 12 cm s^{-1} . Despite the high aspect ratio of the PPS3 trap (4.75),
314 and the small mooring line angle deviations, it is likely that episodic increases in current
315 velocities ($> 12 \text{ cm s}^{-1}$) impacted collection efficiency. When integrated over the entire current
316 meter record (October 2011 to April 2012), the resulting flow is consistent with the annual

317 northeastward, low velocity ($\sim 1 \text{ cm s}^{-1}$) geostrophic flow previously reported over the
318 central part of the Kerguelen plateau (Park et al., 2008b).

319 The depth of the winter mixed layer (WML) on the Kerguelen Plateau is usually
320 shallower than 250 m (Park et al., 1998; Metzl et al., 2006). The sediment trap deployment
321 depth of ~ 300 m was selected to sample particle flux exiting the WML. The moored CTD
322 sensor did not record any evidence of a winter water incursion during the deployment period,
323 confirming the WML did not reach the trap depth. The small depth variations observed during
324 the deployment period resulted from vertical displacement of the trap. Variations of σ_0 may
325 have resulted from both vertical displacement of the CTD sensor and possible isopycnal
326 displacements due to strong internal waves that can occur with an amplitude of > 50 m at this
327 depth (Park et al., 2008a). Our measurements demonstrate that isopycnal displacements are
328 consistent with the M2 (moon 2, 12.4 h period) tidal forcing described in physical modeling
329 studies (Maraldi et al., 2009, 2011). Spectral analysis indicates that high frequency tidal
330 currents are the major circulation components. Time-integrated currents suggest that
331 advection is weak and occurs over longer timescale (months). Assuming the current flow
332 measured at the sediment trap deployment depth is representative of the prevailing current
333 under the WML, more than three months are required for particles to leave the plateau from
334 the A3 station, a timescale larger than the bloom duration itself. Therefore we consider that
335 the particles collected in the sediment trap at station A3 were produced in the surface waters
336 located above the plateau during bloom conditions.

337 **4.2 Swimmers and particle solubilization**

338 Aside from the hydrodynamic effects discussed above, other potential biases characterizing
339 sediment trap deployments, particularly those in shallow waters, is the presence of swimmers
340 and particle solubilization. Swimmers can artificially increase POC fluxes by entering the

341 cups and releasing particulate organic matter or decrease the flux by feeding in the trap funnel
342 (Buesseler et al., 2007a). Some studies have focused specifically on swimmer communities
343 collected in shallow sediment traps (Matsuno et al., 2014 and references therein) although trap
344 collection of swimmers is probably selective and therefore not quantitative. Total swimmer
345 intrusion rate was highest in cups #6 to #9 (December 2011 to February 2012) generally
346 through the representation of copepods and amphipods (Table 2). The maximum swimmer
347 intrusion rate in mid-summer as well as the copepod dominance is consistent with the fourfold
348 increase in mesozooplankton abundance observed from winter to summer (Carlotti et al.,
349 2014). Swimmer abundance was not correlated with mass flux, POC or PON fluxes,
350 suggesting that their presence did not systematically affect particulate fluxes inside the cups.
351 Nevertheless such correlations cannot rule out the possibility of swimmers feeding in the trap
352 funnel modifying particle flux collection.

353 Particle solubilization in preservative solutions may also lead to an underestimation of
354 total flux measured in sediment traps. Previous analyses from traps poisoned with mercuric
355 chloride suggest that ~30 % of total organic carbon flux can be found in the dissolved phase
356 and much higher values of 50 % and 90 % may be observed for nitrogen and phosphorous,
357 respectively (Antia, 2005; O'Neill et al., 2005). Unfortunately the use of a formaldehyde-
358 based preservative in our trap samples precludes any direct estimate of excess of dissolved
359 organic carbon in the sample cup supernatant. Furthermore, corrections for particle leaching
360 have been considered problematic in the presence of swimmers since a fraction of the
361 leaching may originate from the swimmers themselves (Antia, 2005), potentially leading to
362 over-correction. Particle~~s~~ solubilization may have occurred in our samples as evidenced by
363 excess PO_4^{3-} in the supernatant. However the largest values were measured in sample cups
364 where total swimmers were abundant (cups #8 to #12, data not shown). Consequently, it was
365 not possible to discriminate solubilisation of P from swimmers and passively settling particles

366 and it therefore remains difficult to quantify the effect of particle leaching. However, leaching
367 of POC should be less problematic in formalin-preserved samples because aldehydes fix
368 organic matter, ~~rather than in addition to~~ poisoning microbial activity.

369 **4.3 Seasonal dynamics of POC export**

370 The sediment trap record obtained from station A3 provides the first direct estimate of POC
371 export covering an entire season over the naturally fertilized Kerguelen Plateau. We observed
372 a temporal lag of one month between the two surface chlorophyll *a* peaks and the two export
373 events. Based on a compilation of annual sediment trap deployments, Lutz et al. (2007)
374 reported that export quickly follows primary production at low latitudes whereas a time lag up
375 to two months could occur at higher latitudes. A 1-2 month lag was observed between
376 production and export in the pacific sector of the Southern Ocean (Buesseler et al., 2001), as
377 well as along 170°W (Honjo et al., 2000) and in the Australian sector of the Subantarctic
378 Zone (Rigual-Hernández et al., 2015). The temporal lag between surface production and
379 measured export in deep traps can originate~~s~~ from ecological processes in the upper ocean
380 (e.g. carbon retention in the mixed layer) as well as slow sinking velocities (Armstrong et al.,
381 2009) and one cannot differentiate the two processes from a single deep trap signal. A global-
382 scale modeling study suggests that the strongest temporal decoupling between production and
383 export (more than one month) occurs in areas characterized by a strong seasonal variability in
384 primary production (Henson et al., 2014). The study attributes this decoupling to differences
385 in phenology of phytoplankton and zooplankton and evokes zooplankton ejection products as
386 major contributors to fast sinking particles sedimenting post bloom.

387 On the Kerguelen Plateau there is evidence that a significant fraction of
388 phytoplankton biomass comprising the two chlorophyll peaks is remineralized by a highly
389 active heterotrophic microbial community (Obernosterer et al., 2008; Christaki et al., 2014).
390 Another fraction ~~is~~ likely ~~is~~ channeled toward higher trophic levels through the intense

391 grazing pressure that support the observed increase in zooplankton biomass (Carlotti et al.,
392 2008, 2014). Therefore an important fraction of phytoplankton biomass increases observed by
393 satellite may not contribute to export fluxes. Notably, the POC:PON ratio measured in our
394 trap material is close to values reported for marine diatoms (7.3 ± 1.2 , Sarthou et al., 2005),
395 compared to the C:N ratio of zooplankton faecal pellets which is typically higher (7.3 to >15 ,
396 Gerber and Gerber, 1979; Checkley and Entzeroth, 1985; Morales, 1987). Simple mass
397 balance would therefore suggest a significant contribution of phytoplanktonic cells to the
398 POC export, which is indeed corroborated by detailed microscopic analysis (Rembauville et
399 al., 2014).

400 Although we observed increasing contribution of faecal pellet carbon post-bloom
401 (Rembauville et al., 2014), in line with the model output of Henson et al. (2014), differences
402 in phytoplankton and zooplankton phenology do not fully explain the seasonality of export on
403 the Kerguelen Plateau. Considering the shallow trap depth (289 m) and typical sinking speed
404 of 100 m d^{-1} for phyto-aggregates (Allredge and Gotschalk, 1988; Peterson et al., 2005; Trull
405 et al., 2008a), aggregate-driven export following bloom demise would suggest a short lag of a
406 few days between production and export peaks. The temporal lag of one month measured in
407 the present study suggest either slow sinking rates ($<5 \text{ m d}^{-1}$) characteristic of single
408 phytoplanktonic cells or faster sinking particles that ~~do not originate from the peaks of surface~~
409 ~~production~~ originate from sub-surface production peaks undetected by satellite. It is generally
410 accepted that satellite detection depth is 20-50 m (Gordon and McCluney, 1975), ~~and can be~~
411 ~~less than 20 m when surface chlorophyll *a* exceed $0.2 \mu\text{g L}^{-1}$ (Smith, 1981)~~, which prevents
412 the detection of deep phytoplanktonic biomass structures (Villareal et al., 2011). Although
413 subsurface chlorophyll maximum located around 100 m have been observed over the
414 Kerguelen Plateau at the end of the productive period, they have been interpreted to result
415 from the accumulation of surface production at the base of the mixed layer rather than a

416 subsurface productivity feature (Uitz et al., 2009). In support of this detailed taxonomic
417 analysis of the exported material highlight diatom resting spores as major contributors to the
418 two export fluxes rather than a composite surface community accumulated at the base of the
419 mixed layer. The hypothesis of a mass production of nutrient-limited resting spores post-
420 bloom with high settling rates explains the temporal patterns of export we observed
421 (Rembauville et al., 2014). However a better knowledge of the dynamics of factors
422 responsible for resting spore formation by diatoms remains necessary to fully validate this
423 hypothesis.

424 **4.4 Rapid Evidence for significant flux attenuation over the Kerguelen Plateau**

425 The Kerguelen Plateau annual POC export ($98.2 \pm 4.4 \text{ mmol m}^{-2} \text{ y}^{-1}$) approaches the median
426 global ocean POC export value comprising shallow and deep sediment traps ($83 \text{ mmol m}^{-2} \text{ y}^{-1}$,
427 Lampitt and Antia, 1997), but is also close to values observed in HNLC areas of the POOZ
428 ($11\text{--}43 \text{ mmol m}^{-2} \text{ y}^{-1}$ at 500 m, Fischer et al., 2000). Moreover, the magnitude of annual POC
429 export measured at ~300m on the Kerguelen Plateau is comparable to deep-ocean (>2 km)
430 POC fluxes measured from the iron-fertilized Crozet ($60 \text{ mmol m}^{-2} \text{ y}^{-1}$, Salter et al., 2012) and
431 South Georgia blooms ($180 \text{ mmol m}^{-2} \text{ y}^{-1}$, Manno et al., 2014).

432 ~~The annual POC export of $0.1 \text{ mol m}^{-2} \text{ y}^{-1}$ at 289 m (Table 1) represents only 2% of~~
433 ~~the indirect estimate of POC export ($5.1 \text{ mol m}^{-2} \text{ y}^{-1}$) at the base of the WML (200 m) on the~~
434 ~~Kerguelen Plateau based on a seasonal DIC budget (Blain et al., 2007). On shorter time~~
435 ~~scales, the POC flux recorded in the moored sediment trap represents only a small fraction (3~~
436 ~~8%) of the POC flux at the base of the winter mixed layer (200 m) measured by different~~
437 ~~methods during KEOPS2 (Table 3). The same conclusion is true when considering the~~
438 ~~comparison with different estimates made during KEOPS1. The diversity of the methods and~~
439 ~~the difference in the depth where the POC flux was estimated render quantitative comparisons~~
440 ~~challenging, but it appears the POC fluxes measured at 289 m with the moored sediment trap~~

441 ~~are considerably lower than some other estimates. This result indicates either extremely rapid~~
442 ~~attenuation of flux between 200 m and 300 m or major sampling bias by the sediment trap.~~

443 We first compared the sediment trap export fluxes with short-term estimates at 200 m
444 in spring (KEOPS2) and summer (KEOPS1). The POC flux recorded in the moored sediment
445 trap represents only a small fraction (3-8%) of the POC flux measured at the base of the
446 winter mixed layer (200 m) by different approaches during the srping KEOPS2 cruise (Table
447 3). The same conclusion can be drawn when considering the comparison with different
448 estimates made at the end of summer during KEOPS1. Moreover, the annual POC export of
449 $\sim 0.1 \text{ mol m}^{-2} \text{ y}^{-1}$ at 289 m (Table 1) represents only 2% of the indirect estimate of POC export
450 ($5.1 \text{ mol m}^{-2} \text{ y}^{-1}$) at the base of the WML (200 m) on the Kerguelen Plateau based on a
451 seasonal DIC budget (Blain et al., 2007). The short term estimates are derived from a diverse
452 range of methods. The ^{234}Th proxy is based on the ^{234}Th deficit relative to the ^{238}U due to its
453 adsorption on particles, and it subsequent conversion to carbon fluxes using measured
454 POC: ^{234}Th ratios. (Coale and Bruland, 1985; Buesseler et al., 2006; Savoye et al., 2006). The
455 UVP provides high resolution images of particles ($>52 \mu\text{m}$) and the particle size distribution
456 is then converted to carbon fluxes using an empirical relationship (Guidi et al., 2008; Picheral
457 et al., 2010). Drifting gel traps allows the collection, preservation and imaging of sinking
458 particles ($>71 \mu\text{m}$) that are converted to carbon fluxes using empirical volume:carbon
459 relationship (Ebersbach and Trull, 2008; Ebersbach et al., 2011; Laurenceau-Cornec et al.,
460 2015). Finally, drifting sediment traps are conceptually similar to moored sediment traps but
461 avoid most of the hydrodynamic biases associated with this technique (Buesseler et al.,
462 2007a). The diversity of the methods and differences in depth where the POC flux was
463 estimated render quantitative comparisons challenging. Nevertheless, POC fluxes measured at
464 289 m with the moored sediment trap are considerably lower than other estimates made at 200

465 m. This result indicates either extremely rapid attenuation of flux between 200 m and 300 m
466 or significant sampling bias by the sediment trap.

467 We note that low carbon export fluxes around 300 m have been previously reported on
468 the Kerguelen pPlateau. In spring 2011, UVP derived estimates of POC export at 350 m
469 equals are 0.1 to 0.3 mmol m⁻² d⁻¹ (Table 3), a value close to our reported value of 0.15 mmol
470 m⁻² d⁻¹. In summer 2005, POC export at 330 m from gel trap equals is 0.7 mmol m⁻² d⁻¹
471 (Ebersbach and Trull 2008), which is also close to our value of 1.5 mmol m⁻² d⁻¹. Using the
472 Jouandet et al. (2014) data at 200 m (1.9 mmol m⁻² d⁻¹) and 350 m (0.3 mmol m⁻² d⁻¹) and the
473 Ebersbach and Trull (2008) data at 200 m (5.2 mmol m⁻² d⁻¹) and 330 m (0.7 mmol m⁻² d⁻¹)
474 leads to Martin power law exponents values of 3.3 and 4, respectively. These values are high
475 when compared to the range of 0.4–1.7 that was initially compiled for the global ocean
476 (Buesseler et al., 2007b). However, there is increasing evidence in support of much higher b-
477 values in the Southern Ocean that fall in the range 0.9–3.9 (Lam and Bishop, 2007; Henson et
478 al., 2012; Cavan et al., 2015). Our calculations are thus consistent with emerging observations
479 of significant POC flux attenuation in the Southern Ocean. and support a scenario of strong
480 POC flux attenuation between 200 m and 350 m over the Kerguelen Plateau

481 Using the aforementioned b values (3.3 and 4) and the POC flux derived from ²³⁴Th
482 deficit at 200 m in spring (Planchon et al., 2014), we estimate POC fluxes at 289 m of 0.7 to
483 1.1 mmol m⁻² d⁻¹. The flux measured in our sediment trap (0.15 mmol m⁻² d⁻¹) data represents
484 14 % to 21 % of this calculated flux. Very similar percentages (21 % to 27 %) are found using
485 the POC fluxes derived from the ²³⁴Th deficit in summer (Savoye et al., 2008). Therefore we
486 consider that the moored sediment trap collected ~15–30 % of the ²³⁴Th – derived particle flux
487 equivalent throughout the year. Trap-derived particle fluxes can represent 0.1 to >3 times the
488 ²³⁴Th-derived particles in shallow sediment traps (Buesseler, 1991; Buesseler et al., 1994;
489 Coppola et al., 2002; Gustafsson et al., 2004) and this difference is largely attributed to the

490 sum of hydrodynamic biases and swimmer activities (Buesseler, 1991), although it probably
491 also includes the effect of post-collection particle solubilisation. In the Antarctic Peninsula,
492 ^{234}Th derived POC export was 20 times higher than the fluxes collected by a shallow,
493 cylindrical, moored sediment trap at 170 m (Buesseler et al., 2010). The present deployment
494 context is less extreme (depth of 289 m, mean current speed $<10\text{ cm s}^{-1}$, low tilt angle, high
495 aspect ratio of the cylindrical PPS3 trap) but we consider that hydrodynamics (current speed
496 higher than 12 cm s^{-1} during short tidal-driven events) and possible zooplankton feeding on
497 the trap funnel are potential biases that may explain in part the low fluxes recorded by the
498 moored sediment trap. Therefore the low fluxes observed **likely result from a combined effect**
499 **of likely result from a combination of** collection bias (hydrodynamics and swimmers) and
500 **strong** attenuation of the POC flux between the base of the WML and 300 m. **However, it is**
501 **not possible with the current dataset to isolate a specific explanation for low flux values.**

502 **Despite our conclusion that the moored sediment trap deployment was characterized**
503 **by a low collection efficiency of ~15–30% with reference to ^{234}Th -derived fluxes, the**
504 **numerous lines of evidence discussed above appear to converge on a scenario of rapid flux**
505 **attenuation.** Strong POC flux attenuation over the Kerguelen Plateau compared to the open
506 ocean is also reported by Laurenceau-Cornec et al. (2015) who associate this characteristic to
507 a HBLE scenario and invoke the role of mesozooplankton in the carbon flux attenuation.
508 Between October and November 2011, mesozooplankton biomass in the mixed layer doubled
509 (Carlotti et al., 2014) and summer biomass was twofold higher still (Carlotti et al., 2008).
510 These seasonal patterns are consistent with the maximum swimmer intrusion rate and
511 swimmer diversity observed in summer (Table 2). It has previously been concluded that
512 zooplankton biomass is more tightly coupled to phytoplankton biomass on the plateau
513 compared to oceanic waters, leading to higher secondary production on the plateau (Carlotti et
514 al., 2008, 2014). Further support linking zooplankton dynamics to HBLE environments of

515 iron-fertilized blooms are the findings of Cavan et al. (2015) that documents the lowest export
516 ratio (exported production/primary production) in the most productive, naturally fertilized
517 area downstream of South Georgia. Another important ecosystem feature associated to the
518 HBLE environment of the Kerguelen Plateau, and likely shared by other island-fertilized
519 blooms in the Southern Ocean, is the presence of mesopelagic fishes (myctophid spawning
520 and larvae foraging site, Koubbi et al., 1991, 2001). Mesopelagic fishes can be tightly coupled
521 to lower trophic levels (Saba and Steinberg, 2012) and can play a significant role in carbon
522 flux attenuation (Davison et al., 2013). Although important for carbon budgets it is a
523 compartment often neglected due to the challenge of quantitative sampling approaches. We
524 suggest that the HBLE scenario and large attenuation of carbon flux beneath the WML at
525 Kerguelen may represents the transfer of carbon biomass to higher and mobile trophic groups
526 that fuel large mammal and bird populations rather than the classical remineralization-
527 controlled vertical attenuation characterizing open ocean environments. Although technically
528 challenging, testing this hypothesis should be a focus for future studies in this and similar
529 regions.

530 **5. Conclusion**

531 We have reported the seasonal dynamics of particulate organic carbon (POC) export under the
532 winter mixed layer (289 m) of the naturally iron fertilized and productive central Kerguelen
533 Plateau. Annual POC flux was very remarkably low (98 mmol m^{-2}) and most of it occurred
534 primarily during two episodic (<14 days) flux events exported with a 1 month lag following
535 two surface chlorophyll *a* peaks. Analysis of the hydrological conditions and a comparison
536 with different estimates of POC fluxes in spring and summer at the same station suggests that
537 the sediment trap was subject to possible hydrodynamic and biological biases leading to under
538 collection of particle flux. Nevertheless the low POC export was close to other estimates of
539 deep (>300 m) POC export at the same station and is consistent with high attenuation

540 coefficients reported from other methods. ~~Taken together these data suggest that the low~~
541 ~~fluxes can be explained in part by strong flux attenuation between the winter mixed layer~~
542 ~~depth (~200 m) and the trap depth (~300 m). We invoke mesozooplankton and the activity of~~
543 ~~mesopelagic fishes as possible explanations for efficient carbon retention and/or transfer to~~
544 ~~higher trophic levels at the base of the mixed layer which results in a High Biomass, Low~~
545 ~~Export environment. We invoke heterotrophic microbial activity and mesozooplankton and~~
546 ~~mesopelagic fish activity as possible explanations for efficient carbon flux attenuation and/or~~
547 ~~transfer to higher trophic levels which results in a High Biomass, Low Export environment.~~

548 The biogenic silicon, diatoms assemblages and faecal pellet fluxes are reported in a
549 companion paper that identifies the primary ecological vectors regulating the magnitude of
550 POC export and seasonal patterns in BSi:POC export (Rembauville et al., 2014).

551 **Acknowledgements**

552 We thank the Chief Scientist Prof. Bernard Quéguiner, the Captain Bernard Lassiette and his
553 crew during the KEOPS2 mission on the R/V Marion Dufresne II. We thank Leanne Armand
554 and Tom Trull for their constructive comments, as well as three anonymous reviewers which
555 helped us to improve the manuscript. This work was supported by the French Research
556 program of INSU-CNRS LEFE-CYBER (Les enveloppes fluides et l'environnement – Cycles
557 biogéochimiques, environnement et ressources), the French ANR (Agence Nationale de la
558 Recherche, SIMI-6 program, ANR-10-BLAN-0614), the French CNES (Centre National
559 d'Etudes Spatiales) and the French Polar Institute IPEV (Institut Polaire Paul-Emile Victor).

560 **References**

- 561 Allredge, A.L., Gotschalk, C., 1988. In situ settling behavior of marine snow. *Limnol. Oceanogr.* 33, 339–351.
- 562 Aminot, A., Kerouel, R., 2007. Dosage automatique des nutriments dans les eaux marines: méthodes en flux
563 continu. Ifremer, Plouzané, France.
- 564 Antia, A.N., 2005. Solubilization of particles in sediment traps: revising the stoichiometry of mixed layer export.
565 *Biogeosciences* 2, 189–204. doi:10.5194/bg-2-189-2005
- 566 Armstrong, R.A., Peterson, M.L., Lee, C., Wakeham, S.G., 2009. Settling velocity spectra and the ballast ratio
567 hypothesis. *Deep Sea Res. Part II Top. Stud. Oceanogr.* 56, 1470–1478. doi:10.1016/j.dsr2.2008.11.032
- 568 Arrigo, K.R., Worthen, D., Schnell, A., Lizotte, M.P., 1998. Primary production in Southern Ocean waters. *J.*
569 *Geophys. Res. Oceans* 103, 15587–15600. doi:10.1029/98JC00930
- 570 Baker, E.T., Milburn, H.B., Tennant, D.A., 1988. Field assessment of sediment trap efficiency under varying
571 flow conditions. *J. Mar. Res.* 46, 573–592. doi:10.1357/002224088785113522
- 572 Barbeau, K., Moffett, J.W., Caron, D.A., Croot, P.L., Erdner, D.L., 1996. Role of protozoan grazing in relieving
573 iron limitation of phytoplankton. *Nature* 380, 61–64. doi:10.1038/380061a0
- 574 Batten, S.D., Gower, J.F.R., 2014. Did the iron fertilization near Haida Gwaii in 2012 affect the pelagic lower
575 trophic level ecosystem? *J. Plankton Res.* 36, 925–932. doi:10.1093/plankt/fbu049
- 576 Blain, S., Quéguiner, B., Armand, L., Belviso, S., Bomblé, B., Bopp, L., Bowie, A., Brunet, C., Brussaard, C.,
577 Carlotti, F., Christaki, U., Corbière, A., Durand, I., Ebersbach, F., Fuda, J.-L., Garcia, N., Gerringa, L.,
578 Griffiths, B., Guiguer, C., Guillerm, C., Jacquet, S., Jeandel, C., Laan, P., Lefèvre, D., Lo Monaco, C.,
579 Malits, A., Mossner, J., Obernosterer, I., Park, Y.-H., Picheral, M., Pondaven, P., Remenyi, T.,
580 Sandroni, V., Sarthou, G., Savoye, N., Scouarnec, L., Souhaut, M., Thuiller, D., Timmermans, K.,
581 Trull, T., Uitz, J., van Beek, P., Veldhuis, M., Vincent, D., Viollier, E., Vong, L., Wagener, T., 2007.
582 Effect of natural iron fertilization on carbon sequestration in the Southern Ocean. *Nature* 446, 1070–
583 1074. doi:10.1038/nature05700
- 584 Blain, S., Tréguer, P., Belviso, S., Bucciarelli, E., Denis, M., Desabre, S., Fiala, M., Martin Jézéquel, V., Le
585 Fèvre, J., Mayzaud, P., Marty, J.-C., Razouls, S., 2001. A biogeochemical study of the island mass
586 effect in the context of the iron hypothesis: Kerguelen Islands, Southern Ocean. *Deep Sea Res. Part*
587 *Oceanogr. Res. Pap.* 48, 163–187. doi:10.1016/S0967-0637(00)00047-9
- 588 Boltovskoy, D., 1999. South Atlantic zooplankton. *Backhuys*.
- 589 Bopp, L., Kohfeld, K.E., Le Quéré, C., Aumont, O., 2003. Dust impact on marine biota and atmospheric CO₂
590 during glacial periods. *Paleoceanography* 18, 1046. doi:10.1029/2002PA000810
- 591 Boyd, P.W., Jickells, T., Law, C.S., Blain, S., Boyle, E.A., Buesseler, K.O., Coale, K.H., Cullen, J.J., Baar,
592 H.J.W. de, Follows, M., Harvey, M., Lancelot, C., Levasseur, M., Owens, N.P.J., Pollard, R., Rivkin,
593 R.B., Sarmiento, J., Schoemann, V., Smetacek, V., Takeda, S., Tsuda, A., Turner, S., Watson, A.J.,
594 2007. Mesoscale Iron Enrichment Experiments 1993–2005: Synthesis and Future Directions. *Science*
595 315, 612–617. doi:10.1126/science.1131669
- 596 Boyd, P.W., Law, C.S., Hutchins, D.A., Abraham, E.R., Croot, P.L., Ellwood, M., Frew, R.D., Hadfield, M.,
597 Hall, J., Handy, S., Hare, C., Higgins, J., Hill, P., Hunter, K.A., LeBlanc, K., Maldonado, M.T., McKay,
598 R.M., Mioni, C., Oliver, M., Pickmere, S., Pinkerton, M., Safi, K., Sander, S., Sanudo-Wilhelmy, S.A.,
599 Smith, M., Strzepek, R., Tovar-Sanchez, A., Wilhelm, S.W., 2005. FeCycle: Attempting an iron
600 biogeochemical budget from a mesoscale SF₆ tracer experiment in unperturbed low iron waters. *Glob.*
601 *Biogeochem. Cycles* 19, GB4S20. doi:10.1029/2005GB002494
- 602 Boyd, P.W., Trull, T.W., 2007. Understanding the export of biogenic particles in oceanic waters: Is there
603 consensus? *Prog. Oceanogr.* 72, 276–312. doi:10.1016/j.pocean.2006.10.007
- 604 Buesseler, K.O., 1991. Do upper-ocean sediment traps provide an accurate record of particle flux? *Nature* 353,
605 420–423. doi:10.1038/353420a0
- 606 Buesseler, K.O., Antia, A.N., Chen, M., Fowler, S.W., Gardner, W.D., Gustafsson, Ö., Harada, K., Michaels,
607 A.F., Rutgers v. d. Loeff, M., Sarin, M., Steinberg, D.K., Trull, T., 2007a. An assessment of the use of
608 sediment traps for estimating upper ocean particle fluxes. *J. Mar. Res.* 65, 345–416.
- 609 Buesseler, K.O., Ball, L., Andrews, J., Cochran, J.K., Hirschberg, D.J., Bacon, M.P., Fleer, A., Brzezinski, M.,
610 2001. Upper ocean export of particulate organic carbon and biogenic silica in the Southern Ocean along
611 170°W. *Deep Sea Res. Part II Top. Stud. Oceanogr.* 48, 4275–4297. doi:10.1016/S0967-
612 0645(01)00089-3
- 613 Buesseler, K.O., Benitez-Nelson, C.R., Moran, S.B., Burd, A., Charette, M., Cochran, J.K., Coppola, L., Fisher,
614 N.S., Fowler, S.W., Gardner, W.D., Guo, L.D., Gustafsson, Ö., Lamborg, C., Masque, P., Miquel, J.C.,
615 Passow, U., Santschi, P.H., Savoye, N., Stewart, G., Trull, T., 2006. An assessment of particulate
616 organic carbon to thorium-234 ratios in the ocean and their impact on the application of 234Th as a
617 POC flux proxy. *Mar. Chem., Future Applications of 234Th in Aquatic Ecosystems (FATE)* 100, 213–
618 233. doi:10.1016/j.marchem.2005.10.013

- 619 Buesseler, K.O., Boyd, P.W., 2009. Shedding light on processes that control particle export and flux attenuation
620 in the twilight zone of the open ocean. *Limnol. Oceanogr.* 54, 1210–1232.
621 doi:10.4319/lo.2009.54.4.1210
- 622 Buesseler, K.O., Lamborg, C.H., Boyd, P.W., Lam, P.J., Trull, T.W., Bidigare, R.R., Bishop, J.K.B., Casciotti,
623 K.L., Dehairs, F., Elskens, M., Honda, M., Karl, D.M., Siegel, D.A., Silver, M.W., Steinberg, D.K.,
624 Valdes, J., Mooy, B.V., Wilson, S., 2007b. Revisiting Carbon Flux Through the Ocean's Twilight Zone.
625 *Science* 316, 567–570. doi:10.1126/science.1137959
- 626 Buesseler, K.O., McDonnell, A.M.P., Schofield, O.M.E., Steinberg, D.K., Ducklow, H.W., 2010. High particle
627 export over the continental shelf of the west Antarctic Peninsula. *Geophys. Res. Lett.* 37, L22606.
628 doi:10.1029/2010GL045448
- 629 Buesseler, K.O., Michaels, A.F., Siegel, D.A., Knap, A.H., 1994. A three dimensional time-dependent approach
630 to calibrating sediment trap fluxes. *Glob. Biogeochem. Cycles* 8, 179–193. doi:10.1029/94GB00207
- 631 Carlotti, F., Thibault-Botha, D., Nowaczyk, A., Lefèvre, D., 2008. Zooplankton community structure, biomass
632 and role in carbon fluxes during the second half of a phytoplankton bloom in the eastern sector of the
633 Kerguelen Shelf (January–February 2005). *Deep Sea Res. Part II Top. Stud. Oceanogr.* 55, 720–733.
634 doi:10.1016/j.dsr2.2007.12.010
- 635 Cavan, E.L., Le Moigne, F. a. c., Poulton, A.J., Tarling, G.A., Ward, P., Daniels, C.J., Fragoso, G., Sanders, R.J.,
636 2015. Zooplankton fecal pellets control the attenuation of particulate organic carbon flux in the Scotia
637 Sea, Southern Ocean. *Geophys. Res. Lett.* 2014GL062744. doi:10.1002/2014GL062744
- 638 Checkley, D.M., Entzeroth, L.C., 1985. Elemental and isotopic fractionation of carbon and nitrogen by marine,
639 planktonic copepods and implications to the marine nitrogen cycle. *J. Plankton Res.* 7, 553–568.
640 doi:10.1093/plankt/7.4.553
- 641 Christaki, U., Lefèvre, D., Georges, C., Colombet, J., Catala, P., Courties, C., Sime-Ngando, T., Blain, S.,
642 Obernosterer, I., 2014. Microbial food web dynamics during spring phytoplankton blooms in the
643 naturally iron-fertilized Kerguelen area (Southern Ocean). *Biogeosciences* 11, 6739–6753.
644 doi:10.5194/bg-11-6739-2014
- 645 Coale, K.H., Bruland, K.W., 1985. ^{234}Th : ^{238}U Disequilibria Within the California Current. *Limnol.*
646 *Oceanogr.* 30, 22–33.
- 647 Coale, K.H., Johnson, K.S., Chavez, F.P., Buesseler, K.O., Barber, R.T., Brzezinski, M.A., Cochlan, W.P.,
648 Millero, F.J., Falkowski, P.G., Bauer, J.E., Wanninkhof, R.H., Kudela, R.M., Altabet, M.A., Hales,
649 B.E., Takahashi, T., Landry, M.R., Bidigare, R.R., Wang, X., Chase, Z., Strutton, P.G., Friederich,
650 G.E., Gorbunov, M.Y., Lance, V.P., Hilting, A.K., Hiscock, M.R., Demarest, M., Hiscock, W.T.,
651 Sullivan, K.F., Tanner, S.J., Gordon, R.M., Hunter, C.N., Elrod, V.A., Fitzwater, S.E., Jones, J.L.,
652 Tozzi, S., Koblizek, M., Roberts, A.E., Herndon, J., Brewster, J., Ladizinsky, N., Smith, G., Cooper, D.,
653 Timothy, D., Brown, S.L., Selph, K.E., Sheridan, C.C., Twining, B.S., Johnson, Z.I., 2004. Southern
654 Ocean Iron Enrichment Experiment: Carbon Cycling in High- and Low-Si Waters. *Science* 304, 408–
655 414. doi:10.1126/science.1089778
- 656 Coppola, L., Roy-Barman, M., Wassmann, P., Mulsow, S., Jeandel, C., 2002. Calibration of sediment traps and
657 particulate organic carbon export using ^{234}Th in the Barents Sea. *Mar. Chem.* 80, 11–26.
658 doi:10.1016/S0304-4203(02)00071-3
- 659 Davison, P.C., Checkley Jr., D.M., Koslow, J.A., Barlow, J., 2013. Carbon export mediated by mesopelagic
660 fishes in the northeast Pacific Ocean. *Prog. Oceanogr.* 116, 14–30. doi:10.1016/j.pocean.2013.05.013
- 661 De Baar, H.J.W., Boyd, P.W., Coale, K.H., Landry, M.R., Tsuda, A., Assmy, P., Bakker, D.C.E., Bozec, Y.,
662 Barber, R.T., Brzezinski, M.A., Buesseler, K.O., Boyé, M., Croot, P.L., Gervais, F., Gorbunov, M.Y.,
663 Harrison, P.J., Hiscock, W.T., Laan, P., Lancelot, C., Law, C.S., Levasseur, M., Marchetti, A., Millero,
664 F.J., Nishioka, J., Nojiri, Y., van Oijen, T., Riebesell, U., Rijkenberg, M.J.A., Saito, H., Takeda, S.,
665 Timmermans, K.R., Veldhuis, M.J.W., Waite, A.M., Wong, C.-S., 2005. Synthesis of iron fertilization
666 experiments: From the Iron Age in the Age of Enlightenment. *J. Geophys. Res. Oceans* 110, C09S16.
667 doi:10.1029/2004JC002601
- 668 De Baar, H.J.W., Buma, A.G.J., Nolting, R.F., Cadée, G.C., Jacques, G., Tréguer, P., 1990. On iron limitation of
669 the Southern Ocean: experimental observations in the Weddell and Scotia Seas. *Mar. Ecol. Prog. Ser.*
670 65, 105–122. doi:doi:10.3354/meps065105
- 671 Dilling, L., Alldredge, A.L., 2000. Fragmentation of marine snow by swimming macrozooplankton: A new
672 process impacting carbon cycling in the sea. *Deep Sea Res. Part Oceanogr. Res. Pap.* 47, 1227–1245.
673 doi:10.1016/S0967-0637(99)00105-3
- 674 Dunne, J.P., Sarmiento, J.L., Gnanadesikan, A., 2007. A synthesis of global particle export from the surface
675 ocean and cycling through the ocean interior and on the seafloor. *Glob. Biogeochem. Cycles* 21,
676 GB4006. doi:10.1029/2006GB002907
- 677 Ebersbach, F., Trull, T.W., 2008. Sinking particle properties from polyacrylamide gels during the KERguelen
678 Ocean and Plateau compared Study (KEOPS): Zooplankton control of carbon export in an area of

- 679 persistent natural iron inputs in the Southern Ocean. *Limnol. Oceanogr.* 53, 212–224.
680 doi:10.4319/lo.2008.53.1.0212
- 681 Ebersbach, F., Trull, T.W., Davies, D.M., Bray, S.G., 2011. Controls on mesopelagic particle fluxes in the Sub-
682 Antarctic and Polar Frontal Zones in the Southern Ocean south of Australia in summer—Perspectives
683 from free-drifting sediment traps. *Deep Sea Res. Part II Top. Stud. Oceanogr.* 58, 2260–2276.
684 doi:10.1016/j.dsr2.2011.05.025
- 685 Fischer, G., Ratmeyer, V., Wefer, G., 2000. Organic carbon fluxes in the Atlantic and the Southern Ocean:
686 relationship to primary production compiled from satellite radiometer data. *Deep Sea Res. Part II Top.*
687 *Stud. Oceanogr.* 47, 1961–1997. doi:10.1016/S0967-0645(00)00013-8
- 688 Francois, R., Honjo, S., Krishfield, R., Manganini, S., 2002. Factors controlling the flux of organic carbon to the
689 bathypelagic zone of the ocean. *Glob. Biogeochem. Cycles* 16, 1087. doi:10.1029/2001GB001722
- 690 Gall, M.P., Strzepek, R., Maldonado, M., Boyd, P.W., 2001. Phytoplankton processes. Part 2: Rates of primary
691 production and factors controlling algal growth during the Southern Ocean Iron RElease Experiment
692 (SOIREE). *Deep Sea Res. Part II Top. Stud. Oceanogr.*, The Southern Ocean Iron Release Experiment
693 (SOIREE) 48, 2571–2590. doi:10.1016/S0967-0645(01)00009-1
- 694 Gehlen, M., Bopp, L., Emprin, N., Aumont, O., Heinze, C., Ragueneau, O., 2006. Reconciling surface ocean
695 productivity, export fluxes and sediment composition in a global biogeochemical ocean model.
696 *Biogeosciences* 3, 521–537. doi:10.5194/bg-3-521-2006
- 697 Gerber, R.P., Gerber, M.B., 1979. Ingestion of natural particulate organic matter and subsequent assimilation,
698 respiration and growth by tropical lagoon zooplankton. *Mar. Biol.* 52, 33–43. doi:10.1007/BF00386855
- 699 Giering, S.L.C., Sanders, R., Lampitt, R.S., Anderson, T.R., Tamburini, C., Boutrif, M., Zubkov, M.V., Marsay,
700 C.M., Henson, S.A., Saw, K., Cook, K., Mayor, D.J., 2014. Reconciliation of the carbon budget in the
701 ocean’s twilight zone. *Nature* 507, 480–483. doi:10.1038/nature13123
- 702 Gilman, D.L., Fuglister, F.J., Mitchell, J.M., 1963. On the Power Spectrum of “Red Noise.” *J. Atmospheric Sci.*
703 20, 182–184. doi:10.1175/1520-0469(1963)020<0182:OTPSON>2.0.CO;2
- 704 Gordon, H.R., McCluney, W.R., 1975. Estimation of the depth of sunlight penetration in the sea for remote
705 sensing. *Appl. Opt.* 14, 413–416.
- 706 Gruber, N., Gloor, M., Mikaloff Fletcher, S.E., Doney, S.C., Dutkiewicz, S., Follows, M.J., Gerber, M.,
707 Jacobson, A.R., Joos, F., Lindsay, K., Menemenlis, D., Mouchet, A., Müller, S.A., Sarmiento, J.L.,
708 Takahashi, T., 2009. Oceanic sources, sinks, and transport of atmospheric CO₂. *Glob. Biogeochem.*
709 *Cycles* 23, GB1005. doi:10.1029/2008GB003349
- 710 Guidi, L., Jackson, G.A., Stemmann, L., Miquel, J.C., Picheral, M., Gorsky, G., 2008. Relationship between
711 particle size distribution and flux in the mesopelagic zone. *Deep Sea Res. Part Oceanogr. Res. Pap.* 55,
712 1364–1374. doi:10.1016/j.dsr.2008.05.014
- 713 Gustafsson, O., Andersson, P., Roos, P., Kukulska, Z., Broman, D., Larsson, U., Hajdu, S., Ingri, J., 2004.
714 Evaluation of the collection efficiency of upper ocean sub-photic-layer sediment traps: A 24-month in
715 situ calibration in the open Baltic Sea using ²³⁴Th. *Limnol. Oceanogr. Methods* 2, 62–74.
716 doi:10.4319/lom.2004.2.62
- 717 Hawley, N., 1988. Flow in Cylindrical Sediment Traps. *J. Gt. Lakes Res.* 14, 76–88. doi:10.1016/S0380-
718 1330(88)71534-8
- 719 Henson, S.A., Sanders, R., Madsen, E., 2012. Global patterns in efficiency of particulate organic carbon export
720 and transfer to the deep ocean. *Glob. Biogeochem. Cycles* 26, GB1028. doi:10.1029/2011GB004099
- 721 Henson, S.A., Sanders, R., Madsen, E., Morris, P.J., Le Moigne, F., Quartly, G.D., 2011. A reduced estimate of
722 the strength of the ocean’s biological carbon pump. *Geophys. Res. Lett.* 38, L04606.
723 doi:10.1029/2011GL046735
- 724 Henson, S.A., Yool, A., Sanders, R., 2014. Variability in efficiency of particulate organic carbon export: A
725 model study. *Glob. Biogeochem. Cycles* 29, GB4965. doi:10.1002/2014GB004965
- 726 Hiscock, W.T., Millero, F.J., 2005. Nutrient and carbon parameters during the Southern Ocean iron experiment
727 (SOFeX). *Deep Sea Res. Part Oceanogr. Res. Pap.* 52, 2086–2108. doi:10.1016/j.dsr.2005.06.010
- 728 Honjo, S., Francois, R., Manganini, S., Dymond, J., Collier, R., 2000. Particle fluxes to the interior of the
729 Southern Ocean in the Western Pacific sector along 170°W. *Deep Sea Res. Part II Top. Stud. Oceanogr.*
730 47, 3521–3548. doi:10.1016/S0967-0645(00)00077-1
- 731 Honjo, S., Manganini, S.J., Krishfield, R.A., Francois, R., 2008. Particulate organic carbon fluxes to the ocean
732 interior and factors controlling the biological pump: A synthesis of global sediment trap programs since
733 1983. *Prog. Oceanogr.* 76, 217–285. doi:10.1016/j.pocean.2007.11.003
- 734 Hudson, J.M., Steinberg, D.K., Sutton, T.T., Graves, J.E., Latour, R.J., 2014. Myctophid feeding ecology and
735 carbon transport along the northern Mid-Atlantic Ridge. *Deep Sea Res. Part Oceanogr. Res. Pap.* 93,
736 104–116. doi:10.1016/j.dsr.2014.07.002
- 737 Jacquet, S.H.M., Dehairs, F., Savoye, N., Obernosterer, I., Christaki, U., Monnin, C., Cardinal, D., 2008.
738 Mesopelagic organic carbon remineralization in the Kerguelen Plateau region tracked by biogenic

- 739 particulate Ba. Deep Sea Res. Part II Top. Stud. Oceanogr. 55, 868–879.
740 doi:10.1016/j.dsr2.2007.12.038
- 741 JGOFS Sediment Trap Methods, 1994, in: Protocols for the Joint Global Ocean Flux Study (JGOFS) Core
742 Measurements. Intergovernmental Oceanographic Commission, Scientific Committee on Oceanic
743 Research Manual and Guides, UNESCO, pp. 157–164.
- 744 Jouandet, M.P., Blain, S., Metzl, N., Brunet, C., Trull, T.W., Obernosterer, I., 2008. A seasonal carbon budget
745 for a naturally iron-fertilized bloom over the Kerguelen Plateau in the Southern Ocean. Deep Sea Res.
746 Part II Top. Stud. Oceanogr., KEOPS: Kerguelen Ocean and Plateau compared Study 55, 856–867.
747 doi:10.1016/j.dsr2.2007.12.037
- 748 Jouandet, M.-P., Jackson, G.A., Carlotti, F., Picheral, M., Stemmann, L., Blain, S., 2014. Rapid formation of
749 large aggregates during the spring bloom of Kerguelen Island: observations and model comparisons.
750 Biogeosciences 11, 4393–4406. doi:10.5194/bg-11-4393-2014
- 751 Jouandet, M.-P., Trull, T.W., Guidi, L., Picheral, M., Ebersbach, F., Stemmann, L., Blain, S., 2011. Optical
752 imaging of mesopelagic particles indicates deep carbon flux beneath a natural iron-fertilized bloom in
753 the Southern Ocean. Limnol. Oceanogr. 56, 1130–1140. doi:10.4319/lo.2011.56.3.1130
- 754 Karleskind, P., Lévy, M., Memery, L., 2011. Subduction of carbon, nitrogen, and oxygen in the northeast
755 Atlantic. J. Geophys. Res. Oceans 116, C02025. doi:10.1029/2010JC006446
- 756 Kohfeld, K.E., Quéré, C.L., Harrison, S.P., Anderson, R.F., 2005. Role of Marine Biology in Glacial-Interglacial
757 CO₂ Cycles. Science 308, 74–78. doi:10.1126/science.1105375
- 758 Korb, R.E., Whitehouse, M., 2004. Contrasting primary production regimes around South Georgia, Southern
759 Ocean: large blooms versus high nutrient, low chlorophyll waters. Deep Sea Res. Part Oceanogr. Res.
760 Pap. 51, 721–738. doi:10.1016/j.dsr.2004.02.006
- 761 Koubbi, P., Duhamel, G., Hebert, C., 2001. Seasonal relative abundance of fish larvae inshore at îles Kerguelen,
762 Southern Ocean. Antarct. Sci. 13, 385–392. doi:10.1017/S0954102001000542
- 763 Koubbi, P., Ibanez, F., Duhamel, G., 1991. Environmental influences on spatio-temporal oceanic distribution of
764 ichthyoplankton around the Kerguelen Islands (Southern Ocean). Mar. Ecol. Prog. Ser. 72, 225–238.
- 765 Lampitt, R.S., Antia, A.N., 1997. Particle flux in deep seas: regional characteristics and temporal variability.
766 Deep Sea Res. Part Oceanogr. Res. Pap. 44, 1377–1403. doi:10.1016/S0967-0637(97)00020-4
- 767 Lampitt, R.S., Boorman, B., Brown, L., Lucas, M., Salter, I., Sanders, R., Saw, K., Seeyave, S., Thomalla, S.J.,
768 Turnewitsch, R., 2008. Particle export from the euphotic zone: Estimates using a novel drifting
769 sediment trap, 234Th and new production. Deep Sea Res. Part Oceanogr. Res. Pap. 55, 1484–1502.
770 doi:10.1016/j.dsr.2008.07.002
- 771 Lam, P.J., Bishop, J.K.B., 2007. High biomass, low export regimes in the Southern Ocean. Deep Sea Res. Part II
772 Top. Stud. Oceanogr. 54, 601–638. doi:10.1016/j.dsr2.2007.01.013
- 773 Lam, P.J., Doney, S.C., Bishop, J.K.B., 2011. The dynamic ocean biological pump: Insights from a global
774 compilation of particulate organic carbon, CaCO₃, and opal concentration profiles from the
775 mesopelagic. Glob. Biogeochem. Cycles 25, GB3009. doi:10.1029/2010GB003868
- 776 Landry, M.R., Constantinou, J., Latasa, M., Brown, S.L., Bidigare, R.R., Ondrusek, M.E., 2000. Biological
777 response to iron fertilization in the eastern equatorial Pacific (IronEx II). III. Dynamics of
778 phytoplankton growth and microzooplankton grazing. Mar. Ecol. Prog. Ser. 201, 57–72.
779 doi:10.3354/meps201057
- 780 Laurenceau-Cornec, E.C., Trull, T.W., Davies, D.M., Bray, S.G., Doran, J., Planchon, F., Carlotti, F., Jouandet,
781 M.-P., Cavagna, A.-J., Waite, A.M., Blain, S., 2015. The relative importance of phytoplankton
782 aggregates and zooplankton fecal pellets to carbon export: insights from free-drifting sediment trap
783 deployments in naturally iron-fertilised waters near the Kerguelen Plateau. Biogeosciences 12, 1007–
784 1027. doi:10.5194/bg-12-1007-2015
- 785 Laws, E.A., D'Sa, E., Naik, P., 2011. Simple equations to estimate ratios of new or export production to total
786 production from satellite-derived estimates of sea surface temperature and primary production. Limnol.
787 Oceanogr. Methods 593–601. doi:10.4319/lom.2011.9.593
- 788 Laws, E.A., Falkowski, P.G., Smith, W.O., Ducklow, H., McCarthy, J.J., 2000. Temperature effects on export
789 production in the open ocean. Glob. Biogeochem. Cycles 14, 1231–1246. doi:10.1029/1999GB001229
- 790 Lefèvre, D., Guigue, C., Obernosterer, I., 2008. The metabolic balance at two contrasting sites in the Southern
791 Ocean: The iron-fertilized Kerguelen area and HNLC waters. Deep Sea Res. Part II Top. Stud.
792 Oceanogr., KEOPS: Kerguelen Ocean and Plateau compared Study 55, 766–776.
793 doi:10.1016/j.dsr2.2007.12.006
- 794 Le Moigne, F.A.C., Sanders, R.J., Villa-Alfageme, M., Martin, A.P., Pabortsava, K., Planquette, H., Morris, P.J.,
795 Thomalla, S.J., 2012. On the proportion of ballast versus non-ballast associated carbon export in the
796 surface ocean. Geophys. Res. Lett. 39, L15610. doi:10.1029/2012GL052980
- 797 Lenton, A., Tilbrook, B., Law, R.M., Bakker, D., Doney, S.C., Gruber, N., Ishii, M., Hoppema, M., Lovenduski,
798 N.S., Matear, R.J., McNeil, B.I., Metzl, N., Mikaloff Fletcher, S.E., Monteiro, P.M.S., Rödenbeck, C.,

- 799 Sweeney, C., Takahashi, T., 2013. Sea-air CO₂ fluxes in the Southern Ocean for the period 1990–2009.
800 Biogeosciences 10, 4037–4054. doi:10.5194/bg-10-4037-2013
- 801 Le Quéré, C., Andres, R.J., Boden, T., Conway, T., Houghton, R.A., House, J.I., Marland, G., Peters, G.P., van
802 der Werf, G.R., Ahlström, A., Andrew, R.M., Bopp, L., Canadell, J.G., Ciais, P., Doney, S.C., Enright,
803 Friedlingstein, P., Huntingford, C., Jain, A.K., Jourdain, C., Kato, E., Keeling, R.F., Klein
804 Goldewijk, K., Levis, S., Levy, P., Lomas, M., Poulter, B., Raupach, M.R., Schwinger, J., Sitch, S.,
805 Stocker, B.D., Viovy, N., Zaehle, S., Zeng, N., 2013. The global carbon budget 1959–2011. *Earth Syst.*
806 *Sci. Data* 5, 165–185. doi:10.5194/essd-5-165-2013
- 807 Levy, M., Bopp, L., Karleskind, P., Resplandy, L., Ethe, C., Pinsard, F., 2013. Physical pathways for carbon
808 transfers between the surface mixed layer and the ocean interior. *Glob. Biogeochem. Cycles* 27, 1001–
809 1012. doi:10.1002/gbc.20092
- 810 Lima, I.D., Lam, P.J., Doney, S.C., 2014. Dynamics of particulate organic carbon flux in a global ocean model.
811 Biogeosciences 11, 1177–1198. doi:10.5194/bg-11-1177-2014
- 812 Lutz, M.J., Caldeira, K., Dunbar, R.B., Behrenfeld, M.J., 2007. Seasonal rhythms of net primary production and
813 particulate organic carbon flux to depth describe the efficiency of biological pump in the global ocean.
814 *J. Geophys. Res. Oceans* 112, C10011. doi:10.1029/2006JC003706
- 815 Maiti, K., Charette, M.A., Buesseler, K.O., Kahru, M., 2013. An inverse relationship between production and
816 export efficiency in the Southern Ocean. *Geophys. Res. Lett.* 40, 1557–1561. doi:10.1002/grl.50219
- 817 Manno, C., Stowasser, G., Enderlein, P., Fielding, S., Tarling, G.A., 2014. The contribution of zooplankton
818 faecal pellets to deep carbon transport in the Scotia Sea (Southern Ocean). *Biogeosciences Discuss* 11,
819 16105–16134. doi:10.5194/bgd-11-16105-2014
- 820 Maraldi, C., Lyard, F., Testut, L., Coleman, R., 2011. Energetics of internal tides around the Kerguelen Plateau
821 from modeling and altimetry. *J. Geophys. Res. Oceans* 116, C06004. doi:10.1029/2010JC006515
- 822 Maraldi, C., Mongin, M., Coleman, R., Testut, L., 2009. The influence of lateral mixing on a phytoplankton
823 bloom: Distribution in the Kerguelen Plateau region. *Deep Sea Res. Part Oceanogr. Res. Pap.* 56, 963–
824 973. doi:10.1016/j.dsr.2008.12.018
- 825 Maritorena, S., Siegel, D.A., 2005. Consistent merging of satellite ocean color data sets using a bio-optical
826 model. *Remote Sens. Environ.* 94, 429–440. doi:10.1016/j.rse.2004.08.014
- 827 Martin, J.H., Knauer, G.A., Karl, D.M., Broenkow, W.W., 1987. VERTEX: carbon cycling in the northeast
828 Pacific. *Deep Sea Res. Part Oceanogr. Res. Pap.* 34, 267–285. doi:10.1016/0198-0149(87)90086-0
- 829 Martin, P., van der Loeff, M.R., Cassar, N., Vandromme, P., d' Ovidio, F., Stemmann, L., Rengarajan, R.,
830 Soares, M., González, H.E., Ebersbach, F., Lampitt, R.S., Sanders, R., Barnett, B.A., Smetacek, V.,
831 Naqvi, S.W.A., 2013. Iron fertilization enhanced net community production but not downward particle
832 flux during the Southern Ocean iron fertilization experiment LOHAFEX. *Glob. Biogeochem. Cycles*
833 27, 871–881. doi:10.1002/gbc.20077
- 834 Matsuno, K., Yamaguchi, A., Fujiwara, A., Onodera, J., Watanabe, E., Imai, I., Chiba, S., Harada, N., Kikuchi,
835 T., 2014. Seasonal changes in mesozooplankton swimmers collected by sediment trap moored at a
836 single station on the Northwind Abyssal Plain in the western Arctic Ocean. *J. Plankton Res.* 36, 490–
837 502. doi:10.1093/plankt/fbt092
- 838 Measures, C.I., Brown, M.T., Selph, K.E., Apprill, A., Zhou, M., Hatté, M., Hiscock, W.T., 2013. The influence
839 of shelf processes in delivering dissolved iron to the HNLC waters of the Drake Passage, Antarctica.
840 *Deep Sea Res. Part II Top. Stud. Oceanogr.* 90, 77–88. doi:10.1016/j.dsr2.2012.11.004
- 841 Metzl, N., Brunet, C., Jabaud-Jan, A., Poisson, A., Schauer, B., 2006. Summer and winter air-sea CO₂ fluxes in
842 the Southern Ocean. *Deep Sea Res. Part Oceanogr. Res. Pap.* 53, 1548–1563.
843 doi:10.1016/j.dsr.2006.07.006
- 844 Moore, J.K., Doney, S.C., Lindsay, K., 2004. Upper ocean ecosystem dynamics and iron cycling in a global
845 three-dimensional model. *Glob. Biogeochem. Cycles* 18, GB4028. doi:10.1029/2004GB002220
- 846 Morales, C.E., 1987. Carbon and nitrogen content of copepod faecal pellets: effect of food concentration and
847 feeding behaviour. *Mar. Ecol. Prog. Ser.* 36, 107–114.
- 848 Obernosterer, I., Christaki, U., Lefèvre, D., Catala, P., Van Wambeke, F., Lebaron, P., 2008. Rapid bacterial
849 mineralization of organic carbon produced during a phytoplankton bloom induced by natural iron
850 fertilization in the Southern Ocean. *Deep Sea Res. Part II Top. Stud. Oceanogr.* 55, 777–789.
851 doi:10.1016/j.dsr2.2007.12.005
- 852 O'Neill, L.P., Benitez-Nelson, C.R., Styles, R.M., Tappa, E., Thunell, R.C., 2005. Diagenetic effects on
853 particulate phosphorus samples collected using formalin poisoned sediment traps. *Limnol. Oceanogr.*
854 *Methods* 3, 308–317. doi:10.4319/lom.2005.3.3.308
- 855 Park, Y.-H., Charriaud, E., Pino, D.R., Jeandel, C., 1998. Seasonal and interannual variability of the mixed layer
856 properties and steric height at station KERFIX, southwest of Kerguelen. *J. Mar. Syst.* 17, 571–586.
857 doi:10.1016/S0924-7963(98)00065-7

- 858 Park, Y.-H., Fuda, J.-L., Durand, I., Naveira Garabato, A.C., 2008a. Internal tides and vertical mixing over the
859 Kerguelen Plateau. *Deep Sea Res. Part II Top. Stud. Oceanogr.* 55, 582–593.
860 doi:10.1016/j.dsr2.2007.12.027
- 861 Park, Y.-H., Roquet, F., Durand, I., Fuda, J.-L., 2008b. Large-scale circulation over and around the Northern
862 Kerguelen Plateau. *Deep Sea Res. Part II Top. Stud. Oceanogr.* 55, 566–581.
863 doi:10.1016/j.dsr2.2007.12.030
- 864 Peterson, M.L., Wakeham, S.G., Lee, C., Askea, M.A., Miquel, J.C., 2005. Novel techniques for collection of
865 sinking particles in the ocean and determining their settling rates. *Limnol. Oceanogr. Methods* 3, 520–
866 532. doi:10.4319/lom.2005.3.520
- 867 Picheral, M., Guidi, L., Stemmann, L., Karl, D.M., Iddaoud, G., Gorsky, G., 2010. The Underwater Vision
868 Profiler 5: An advanced instrument for high spatial resolution studies of particle size spectra and
869 zooplankton. *Limnol. Oceanogr. Methods* 8, 462–473. doi:10.4319/lom.2010.8.462
- 870 Planchon, F., Ballas, D., Cavagna, A.-J., Bowie, A.R., Davies, D., Trull, T., Laurenceau, E., Van Der Merwe, P.,
871 Dehairs, F., 2014. Carbon export in the naturally iron-fertilized Kerguelen area of the Southern Ocean
872 based on the ^{234}Th approach. *Biogeosciences Discuss* 11, 15991–16032. doi:10.5194/bgd-11-15991-
873 2014
- 874 Pollard, R., Sanders, R., Lucas, M., Statham, P., 2007. The Crozet Natural Iron Bloom and Export Experiment
875 (CROZEX). *Deep Sea Res. Part II Top. Stud. Oceanogr.* 54, 1905–1914.
876 doi:10.1016/j.dsr2.2007.07.023
- 877 Pollard, R.T., Salter, I., Sanders, R.J., Lucas, M.I., Moore, C.M., Mills, R.A., Statham, P.J., Allen, J.T., Baker,
878 A.R., Bakker, D.C.E., Charette, M.A., Fielding, S., Fones, G.R., French, M., Hickman, A.E., Holland,
879 R.J., Hughes, J.A., Jickells, T.D., Lampitt, R.S., Morris, P.J., Nédélec, F.H., Nielsdóttir, M., Planquette,
880 H., Popova, E.E., Poulton, A.J., Read, J.F., Seeyave, S., Smith, T., Stinchcombe, M., Taylor, S.,
881 Thomalla, S., Venables, H.J., Williamson, R., Zubkov, M.V., 2009. Southern Ocean deep-water carbon
882 export enhanced by natural iron fertilization. *Nature* 457, 577–580. doi:10.1038/nature07716
- 883 Rembauville, M., Blain, S., Armand, L., Quéguiner, B., Salter, I., 2014. Export fluxes in a naturally fertilized
884 area of the Southern Ocean, the Kerguelen Plateau: ecological vectors of carbon and biogenic silica to
885 depth (Part 2). *Biogeosciences Discuss* 11, 17089–17150. doi:10.5194/bgd-11-17089-2014
- 886 Rigual-Hernández, A.S., Trull, T.W., Bray, S.G., Closset, I., Armand, L.K., 2015. Seasonal dynamics in diatom
887 and particulate export fluxes to the deep sea in the Australian sector of the southern Antarctic Zone. *J. Mar. Syst.* 142, 62–74. doi:10.1016/j.jmarsys.2014.10.002
- 888 Rivkin, R.B., Legendre, L., 2001. Biogenic carbon cycling in the upper ocean: effects of microbial respiration.
889 *Science* 291, 2398–2400. doi:10.1126/science.291.5512.2398
- 890 Rynearson, T.A., Richardson, K., Lampitt, R.S., Sieracki, M.E., Poulton, A.J., Lyngsgaard, M.M., Perry, M.J.,
891 2013. Major contribution of diatom resting spores to vertical flux in the sub-polar North Atlantic. *Deep
892 Sea Res. Part Oceanogr. Res. Pap.* 82, 60–71. doi:10.1016/j.dsr.2013.07.013
- 893 Saba, G.K., Steinberg, D.K., 2012. Abundance, Composition, and Sinking Rates of Fish Fecal Pellets in the
894 Santa Barbara Channel. *Sci. Rep.* 2. doi:10.1038/srep00716
- 895 Salter, I., Kemp, A.E.S., Lampitt, R.S., Gledhill, M., 2010. The association between biogenic and inorganic
896 minerals and the amino acid composition of settling particles. *Limnol. Oceanogr.* 55, 2207–2218.
897 doi:10.4319/lo.2010.55.5.2207
- 898 Salter, I., Kemp, A.E.S., Moore, C.M., Lampitt, R.S., Wolff, G.A., Holtvoeth, J., 2012. Diatom resting spore
899 ecology drives enhanced carbon export from a naturally iron-fertilized bloom in the Southern Ocean.
900 *Glob. Biogeochem. Cycles* 26, GB1014. doi:10.1029/2010GB003977
- 901 Salter, I., Lampitt, R.S., Sanders, R., Poulton, A., Kemp, A.E.S., Boorman, B., Saw, K., Pearce, R., 2007.
902 Estimating carbon, silica and diatom export from a naturally fertilised phytoplankton bloom in the
903 Southern Ocean using PELAGRA: A novel drifting sediment trap. *Deep Sea Res. Part II Top. Stud.
904 Oceanogr.*, The Crozet Natural Iron Bloom and Export Experiment CROZEX 54, 2233–2259.
905 doi:10.1016/j.dsr2.2007.06.008
- 906 Salter, I., Schiebel, R., Ziveri, P., Movellan, A., Lampitt, R., Wolff, G.A., 2014. Carbonate counter pump
907 stimulated by natural iron fertilization in the Polar Frontal Zone. *Nat. Geosci.* 7, 885–889.
908 doi:10.1038/ngeo2285
- 909 Sarmiento, J.L., Gruber, N., 2006. Ocean Biogeochemical Dynamics. Princeton University Press, Princeton.
- 910 Sarmiento, J.L., Le Quéré, C., 1996. Oceanic Carbon Dioxide Uptake in a Model of Century-Scale Global
911 Warming. *Science* 274, 1346–1350.
- 912 Sarthou, G., Timmermans, K.R., Blain, S., Tréguer, P., 2005. Growth physiology and fate of diatoms in the
913 ocean: a review. *J. Sea Res., Iron Resources and Oceanic Nutrients - Advancement of Global
914 Environmental Simulations* 53, 25–42. doi:10.1016/j.seares.2004.01.007
- 915

- 916 Savoye, N., Benitez-Nelson, C., Burd, A.B., Cochran, J.K., Charette, M., Buesseler, K.O., Jackson, G.A., Roy-
917 Barman, M., Schmidt, S., Elskens, M., 2006. *234*Th sorption and export models in the water column: A
918 review. *Mar. Chem.* 100, 234–249. doi:10.1016/j.marchem.2005.10.014
- 919 Savoye, N., Trull, T.W., Jacquet, S.H.M., Navez, J., Dehairs, F., 2008. *234*Th-based export fluxes during a
920 natural iron fertilization experiment in the Southern Ocean (KEOPS). *Deep Sea Res. Part II Top. Stud.*
921 *Oceanogr.*, KEOPS: Kerguelen Ocean and Plateau compared Study 55, 841–855.
922 doi:10.1016/j.dsr2.2007.12.036
- 923 Schlitzer, R., 2004. Export production in the Equatorial and North Pacific derived from dissolved oxygen,
924 nutrient and carbon data. *J. Oceanogr.* Vol 60 No 1 Pp 53–62.
- 925 Schulz, M., Mudelsee, M., 2002. REDFIT: estimating red-noise spectra directly from unevenly spaced
926 paleoclimatic time series. *Comput. Geosci.* 28, 421–426. doi:10.1016/S0098-3004(01)00044-9
- 927 Seeyave, S., Lucas, M.I., Moore, C.M., Poulton, A.J., 2007. Phytoplankton productivity and community
928 structure in the vicinity of the Crozet Plateau during austral summer 2004/2005. *Deep Sea Res. Part II*
929 *Top. Stud. Oceanogr.*, The Crozet Natural Iron Bloom and Export Experiment CROZEX 54, 2020–
930 2044. doi:10.1016/j.dsr2.2007.06.010
- 931 Smetacek, V., Assmy, P., Henjes, J., 2004. The role of grazing in structuring Southern Ocean pelagic ecosystems
932 and biogeochemical cycles. *Antarct. Sci.* 16, 541–558. doi:10.1017/S0954102004002317
- 933 Smith, R.C., 1981. Remote sensing and depth distribution of ocean chlorophyll. *Mar. Ecol.-Prog. Ser.* 5, 359–
934 361.
- 935 Tarling, G.A., Ward, P., Atkinson, A., Collins, M.A., Murphy, E.J., 2012. DISCOVERY 2010: Spatial and
936 temporal variability in a dynamic polar ecosystem. *Deep Sea Res. Part II Top. Stud. Oceanogr.* 59–60,
937 1–13. doi:10.1016/j.dsr2.2011.10.001
- 938 Thomalla, S.J., Fauchereau, N., Swart, S., Monteiro, P.M.S., 2011. Regional scale characteristics of the seasonal
939 cycle of chlorophyll in the Southern Ocean. *Biogeosciences* 8, 2849–2866. doi:10.5194/bg-8-2849-
940 2011
- 941 Trull, T.W., Bray, S.G., Buesseler, K.O., Lamborg, C.H., Manganini, S., Moy, C., Valdes, J., 2008. In situ
942 measurement of mesopelagic particle sinking rates and the control of carbon transfer to the ocean
943 interior during the Vertical Flux in the Global Ocean (VERTIGO) voyages in the North Pacific. *Deep*
944 *Sea Res. Part II Top. Stud. Oceanogr.* 55, 1684–1695. doi:10.1016/j.dsr2.2008.04.021
- 945 Trull, T.W., Davies, D., Casciotti, K., 2008. Insights into nutrient assimilation and export in naturally iron-
946 fertilized waters of the Southern Ocean from nitrogen, carbon and oxygen isotopes. *Deep Sea Res. Part*
947 *II Top. Stud. Oceanogr.* 55, 820–840. doi:10.1016/j.dsr2.2007.12.035
- 948 Tsuda, A., Takeda, S., Saito, H., Nishioka, J., Kudo, I., Nojiri, Y., Suzuki, K., Uematsu, M., Wells, M.L.,
949 Tsumune, D., Yoshimura, T., Aono, T., Aramaki, T., Cochlan, W.P., Hayakawa, M., Imai, K., Isada, T.,
950 Iwamoto, Y., Johnson, W.K., Kameyama, S., Kato, S., Kiyosawa, H., Kondo, Y., Levasseur, M.,
951 Machida, R.J., Nagao, I., Nakagawa, F., Nakanishi, T., Nakatsuka, S., Narita, A., Noir, Y., Obata, H.,
952 Ogawa, H., Oguma, K., Ono, T., Sakuragi, T., Sasakawa, M., Sato, M., Shimamoto, A., Takata, H.,
953 Trick, C.G., Watanabe, Y.W., Wong, C.S., Yoshie, N., 2007. Evidence for the grazing hypothesis:
954 Grazing reduces phytoplankton responses of the HNLC ecosystem to iron enrichment in the western
955 subarctic pacific (SEEDS II). *J. Oceanogr.* 63, 983–994. doi:10.1007/s10872-007-0082-x
- 956 Uitz, J., Claustre, H., Griffiths, F.B., Ras, J., Garcia, N., Sandroni, V., 2009. A phytoplankton class-specific
957 primary production model applied to the Kerguelen Islands region (Southern Ocean). *Deep Sea Res.*
958 *Part Oceanogr. Res. Pap.* 56, 541–560. doi:10.1016/j.dsr.2008.11.006
- 959 Villareal, T.A., Adornato, L., Wilson, C., Schoenbaechler, C.A., 2011. Summer blooms of diatom-diazotroph
960 assemblages and surface chlorophyll in the North Pacific gyre: A disconnect. *J. Geophys. Res. Oceans*
961 116, C03001. doi:10.1029/2010JC006268
- 962 Volk, T., Hoffert, M.I., 1985. Ocean carbon pumps: Analysis of relative strengths and efficiencies in ocean-
963 driven atmospheric CO₂ changes, in: Sundquist, E.T., Broecker, W.S. (Eds.), *Geophysical Monograph*
964 Series. American Geophysical Union, Washington, D. C., pp. 99–110.
- 965

966 **Table 1:** Dynamics of carbon and nitrogen export fluxes at station A3 collected by the
 967 sediment trap at 289 m.

Cup	Start	Stop	Fluxes (mmol m ⁻² d ⁻¹)			Contribution to annual export (%)	
			POC	PON	POC:PON	POC	PON
1	21/10/2011	04/11/2011	0.15±0.01	0.02±0.00	6.80±0.56	2.11±0.06	2.30±0.01
2	04/11/2011	18/11/2011	0.14 ±0.01	0.02±0.00	6.09±0.67	1.94±0.16	2.27±0.15
3	18/11/2011	02/12/2011	0.15±0.01	0.02±0.00	7.33±0.31	2.12±0.06	1.99±0.06
4	02/12/2011	12/12/2011	1.60±0.04	0.23±0.01	6.95±0.29	16.18±0.45	16.48±0.07
5	12/12/2011	22/12/2011	0.34±0.00	0.05±0.00	6.87±0.08	3.41±0.03	3.64±0.03
6	22/12/2011	01/01/2012	0.51±0.04	0.08±0.01	6.70±0.78	4.82±0.76	5.50±0.39
7	01/01/2012	11/01/2012	0.42±0.02	0.06±0.00	6.73±0.46	4.23±0.14	4.65±0.42
8	11/01/2012	25/01/2012	0.34±0.01	0.05±0.00	6.94±0.38	4.83±0.18	4.84±0.11
9	25/01/2012	08/02/2012	1.47±0.03	0.20±0.01	7.38±0.26	20.98±0.57	21.07±0.05
10	08/02/2012	22/02/2012	0.55±0.04	0.08±0.00	6.97±0.88	7.83±0.64	8.36±0.57
11	22/02/2012	31/05/2012	0.27±0.01	0.03±0.00	8.09±0.22	26.84±0.47	24.12±0.20
12	31/05/2012	07/09/2012	0.04±0.00	0.01±0.00	6.06±0.17	4.71±0.90	4.78±0.09
Annual export (mmol m⁻² y⁻¹)			98.24±4.35	13.59±0.30			

968

969

970 **Table 2:** Number of swimmer individuals found in each cup and swimmer intrusion rate
 971 (number d^{-1} , *bold italic* numbers) for each taxa and for the total swimmers.

Cup	Copepod	Pteropod	Euphausi d	Ostracod	Amphipo d	Cnidaria n	Polychaet e	Ctenopho re	Siphonop hore	Salp	Total
1	166	13	1	2	1	0	0	0	0	0	183
	<i>12</i>	<i>1</i>	<i>< 1</i>	<i>< 1</i>	<i>< 1</i>	<i>0</i>	<i>0</i>	<i>0</i>	<i>0</i>	<i>0</i>	<i>13</i>
2	55	0	0	0	0	0	0	0	0	0	55
	<i>4</i>	<i>0</i>	<i>0</i>	<i>0</i>	<i>0</i>	<i>0</i>	<i>0</i>	<i>0</i>	<i>0</i>	<i>0</i>	<i>4</i>
3	0	0	0	0	0	0	0	0	0	0	0
	<i>0</i>	<i>0</i>	<i>0</i>	<i>0</i>	<i>0</i>	<i>0</i>	<i>0</i>	<i>0</i>	<i>0</i>	<i>0</i>	<i>0</i>
4	113	0	0	0	0	0	0	0	0	0	113
	<i>11</i>	<i>0</i>	<i>0</i>	<i>0</i>	<i>0</i>	<i>0</i>	<i>0</i>	<i>0</i>	<i>0</i>	<i>0</i>	<i>11</i>
5	0	0	0	0	0	0	0	0	0	0	0
	<i>0</i>	<i>0</i>	<i>0</i>	<i>0</i>	<i>0</i>	<i>0</i>	<i>0</i>	<i>0</i>	<i>0</i>	<i>0</i>	<i>0</i>
6	540	0	1	0	2	5	1	4	1	0	554
	<i>54</i>	<i>0</i>	<i>< 1</i>	<i>0</i>	<i>< 1</i>	<i>< 1</i>	<i>0</i>	<i>0</i>	<i>0</i>	<i>0</i>	<i>55</i>
7	583	0	0	0	0	2	2	3	0	0	590
	<i>58</i>	<i>0</i>	<i>0</i>	<i>0</i>	<i>0</i>	<i>< 1</i>	<i>< 1</i>	<i>< 1</i>	<i>0</i>	<i>0</i>	<i>58</i>
8	686	33	2	2	8	5	1	4	0	0	741
	<i>49</i>	<i>2</i>	<i>< 1</i>	<i>< 1</i>	<i>1</i>	<i>< 1</i>	<i>< 1</i>	<i>< 1</i>	<i>0</i>	<i>0</i>	<i>52</i>
9	392	14	4	3	121	4	2	0	0	0	540
	<i>28</i>	<i>1</i>	<i>< 1</i>	<i>< 1</i>	<i>9</i>	<i>< 1</i>	<i>< 1</i>	<i>0</i>	<i>0</i>	<i>0</i>	<i>38</i>
10	264	69	1	2	18	11	0	2	0	0	367
	<i>19</i>	<i>5</i>	<i>< 1</i>	<i>< 1</i>	<i>1</i>	<i>1</i>	<i>0</i>	<i>< 1</i>	<i>0</i>	<i>0</i>	<i>26</i>
11	54	0	0	0	29	4	1	0	0	0	88
	<i>1</i>	<i>0</i>	<i>0</i>	<i>0</i>	<i>< 1</i>	<i>< 1</i>	<i>< 1</i>	<i>0</i>	<i>0</i>	<i>0</i>	<i>1</i>
12	1481	44	5	7	2	3	2	0	0	1	1544
	<i>15</i>	<i>< 1</i>	<i>0</i>	<i>0</i>	<i>< 1</i>	<i>15</i>					

972

973

974 **Table 3:** Synthesis of estimates of POC fluxes at the base of, or under, the mixed layer at
 975 station A3 from the KEOPS 1 cruise.

Author	Method	Period	Depth (m)	POC flux (mmol m ⁻² d ⁻¹)
KEOPS1				
Savoye et al., 2008	²³⁴ Th deficit	23 Jan – 12 Feb 2005	100	23 ± 3.6
			150	25.7 ± 3.6
			200	24.5 ± 6.8
Ebersbach and Trull, 2008	Drifting gel trap, optical measurements and constant C conversion factor	4 Feb 2005 12 Feb 2005	200	23.9
			100	5.3
			200	5.2
			330	0.7
			430	1
Jouandet et al., 2008	Annual DIC budget	Annual	MLD base	85
Trull et al., 2008b	Drifting sediment trap	4 Feb 2005		7.3-10
		12 Feb 2005	200	3-3.1
Jouandet et al., 2011	In situ optical measurement (UVP) and power function C conversion factor	22 Jan 2005	200	72.4
			330	27.2
			400	21.6
			200	29.8
			330	26.8
		23 Jan 2005 12 Feb 2005	400	15.9
			200	4.8
			330	5.6
			400	7.9
KEOPS2				
Planchon et al., 2014	²³⁴ Th deficit, steady state model	20 Oct 2011	100	3.5 ± 0.9
			150	3.9 ± 0.9
			200	3.7 ± 0.9
		16 Nov 2011	100	4.6 ± 1.5
			150	7.1 ± 1.5
			200	3.1 ± 0.6
Jouandet et al., 2014	²³⁴ Th deficit, non steady state model	16 Nov 2011	100	7.3 ± 1.8
			150	8.4 ± 1.8
			200	3.8 ± 0.8
Laurenceau-Cornec et al., 2015	Drifting gel trap, optical measurement of particles	16 Nov 2011	210	5.5
			210	2.2
Jouandet et al., 2014	In situ optical measurement (UVP) and power function C conversion factor	21 Oct 2011	200	0.2
			350	0.1
		16 Nov 2011	200	1.9
			350	0.3

977 **Figures captions**

978 **Figure 1.** Localization of the Kerguelen Plateau in the Indian sector of the Southern Ocean
979 and detailed map of the satellite-derived surface chlorophyll *a* concentration (MODIS level 3
980 product) averaged over the sediment trap deployment period. Sediment trap location at the A3
981 station is represented by a black dot, whereas the black circle represents the 100 km radius
982 area used to average the surface chlorophyll *a* time series. Arrows represent surface
983 geostrophic circulation derived from the absolute dynamic topography (AVISO product).
984 Positions of the Antarctic Circumpolar Current core (AAC core), the Polar Front (PF) and the
985 Fawn Through Current (FTC) are shown by thick black arrows. Grey lines are 500 m and
986 1000 m isobaths.

987 **Figure 2.** Schematic of the instrumented mooring line against vertical temperature profiles.
988 The sediment trap and the current meter/CTD sensor location on the mooring line are shown
989 by white circles. Temperature profiles performed during the sediment trap deployment (20
990 October 2011) are represented by grey lines. Black full line is the median temperature profile
991 from 12 casts realized on the 16 November 2011. Dashed black lines are the first and third
992 quartiles from these casts. The grey rectangle represents the Kerguelen Plateau seafloor. The
993 different water masses are Antarctic Surface Water (AASW), Winter Water (WW) and Upper
994 Circumpolar Deep Water (UCDW).

995 **Figure 3.** Hydrological properties recorded by the instrument mooring at station A3. a) depth
996 of the CTD sensor, b) salinity, c) potential temperature, d) line angle, e) current speed, grey
997 lines are raw data, black lines are low-pass filtered data with a Gaussian filter (40 hour
998 window as suggested by the spectral analysis), f) direction and speed of currents represented
999 by vectors (under sampled with a 5 hours interval) and g) wind rose plot of current direction

1000 and intensities, dotted circles are directions relatives frequencies and colors refer to current
1001 speed (m s^{-1}).

1002 **Figure 4.** Potential temperature/salinity diagram at station A3. Data are from the moored
1003 CTD (black dots), KEOPS1 (blue line) and KEOPS2 (red line). Grey lines are potential
1004 density anomaly. The different water masses are Antarctic Surface Water (AASW), Winter
1005 Water (WW) and Upper Circumpolar Deep Water (UCDW).

1006

1007 **Figure 5.** Power spectrum of the spectral analysis of a) depth time series and b) potential
1008 density anomaly time series. Pure red noise (null hypothesis) is represented by red dashed
1009 lines for each variable. The period corresponding to a significant power peak (power peak
1010 higher than the red noise) is written.

1011 **Figure 6.** Progressive vector diagram (integration of the current vectors all along the current
1012 meter record) calculated from current meter data at 319 m. The color scale refers to date.

1013 **Figure 7.** Seasonal variations of surface chlorophyll *a* and particulate organic carbon (POC)
1014 export. a) Seasonal surface chlorophyll concentration and 16 years climatology (Globcolour)
1015 averaged in a 100 km radius around the station A3 station The black line represents the
1016 climatology calculated for the period 1997/2013, whilst the green line corresponds to the
1017 sediment trap deployment period (2011/2012). b) POC flux (grey bars) and mass percentage
1018 of POC (red dotted line). Error bars are standard deviations from triplicates, bold italic
1019 numbers refer to cup number.

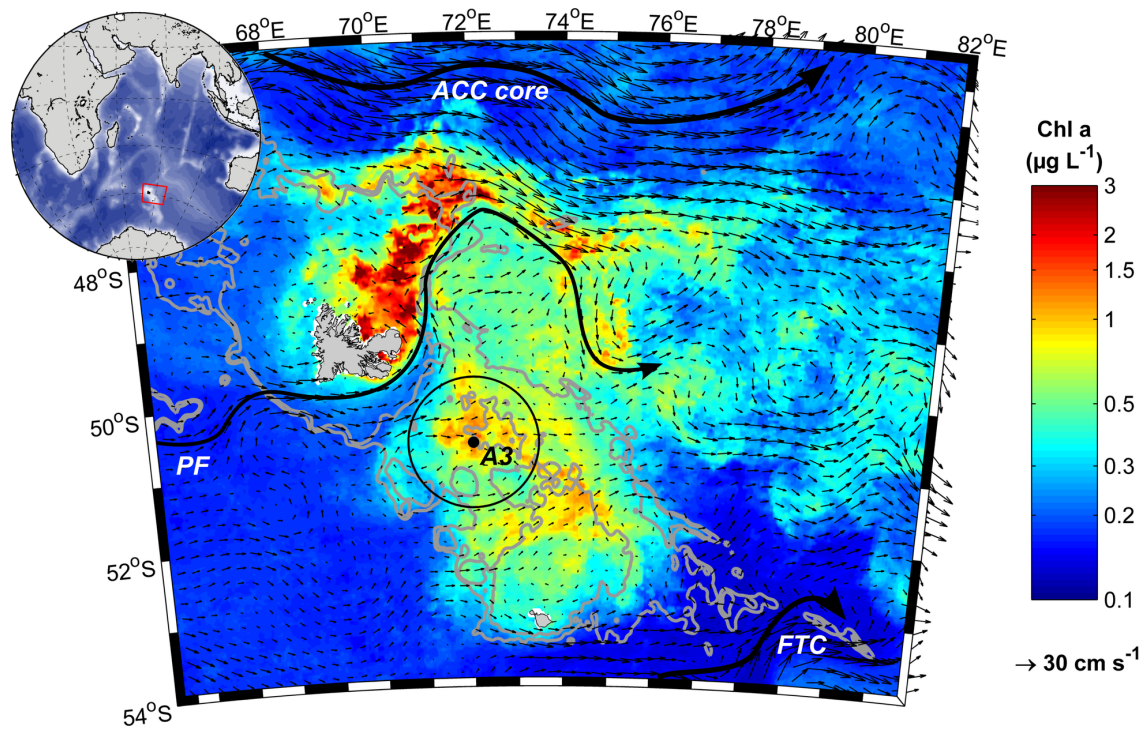


Figure 1.

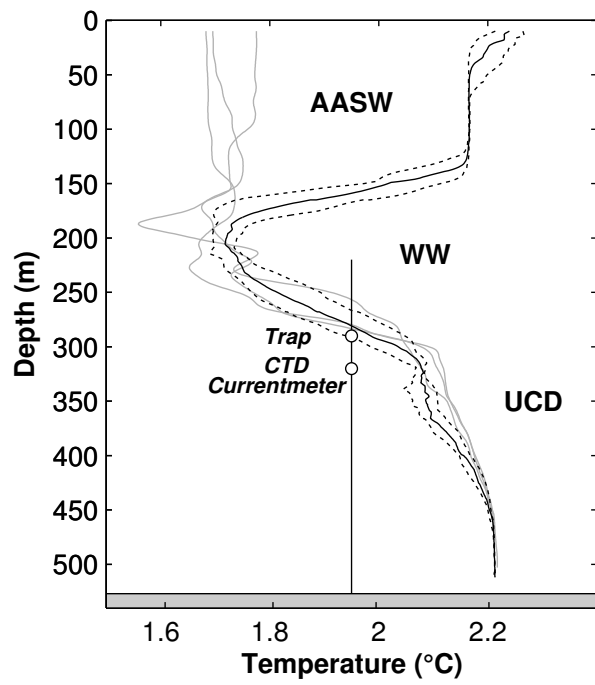


Figure 2.

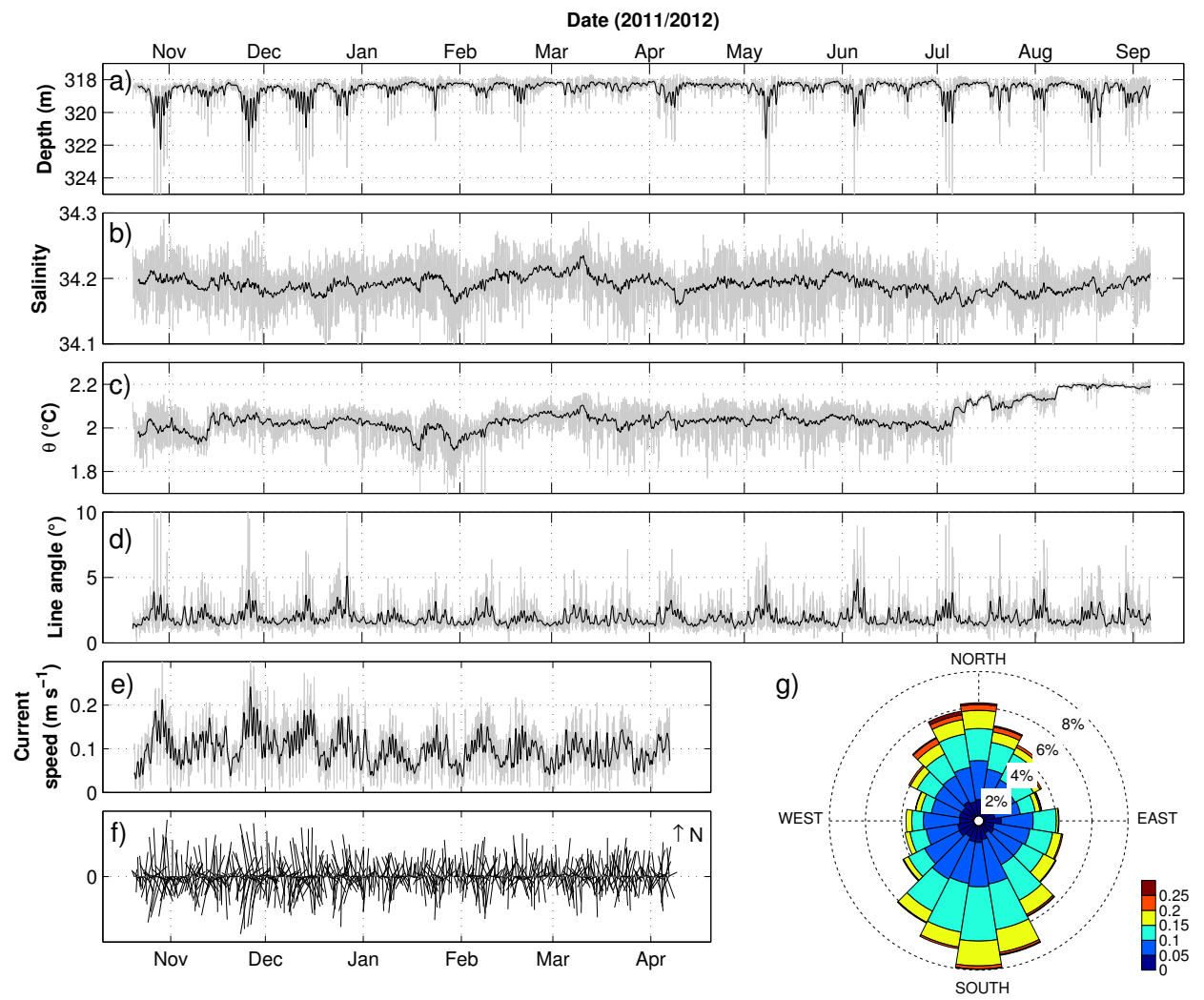


Figure 3.

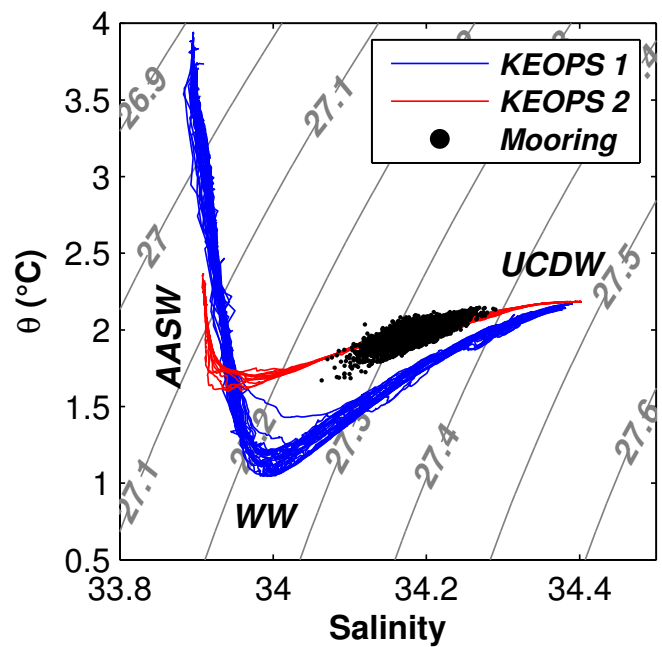


Figure 4.

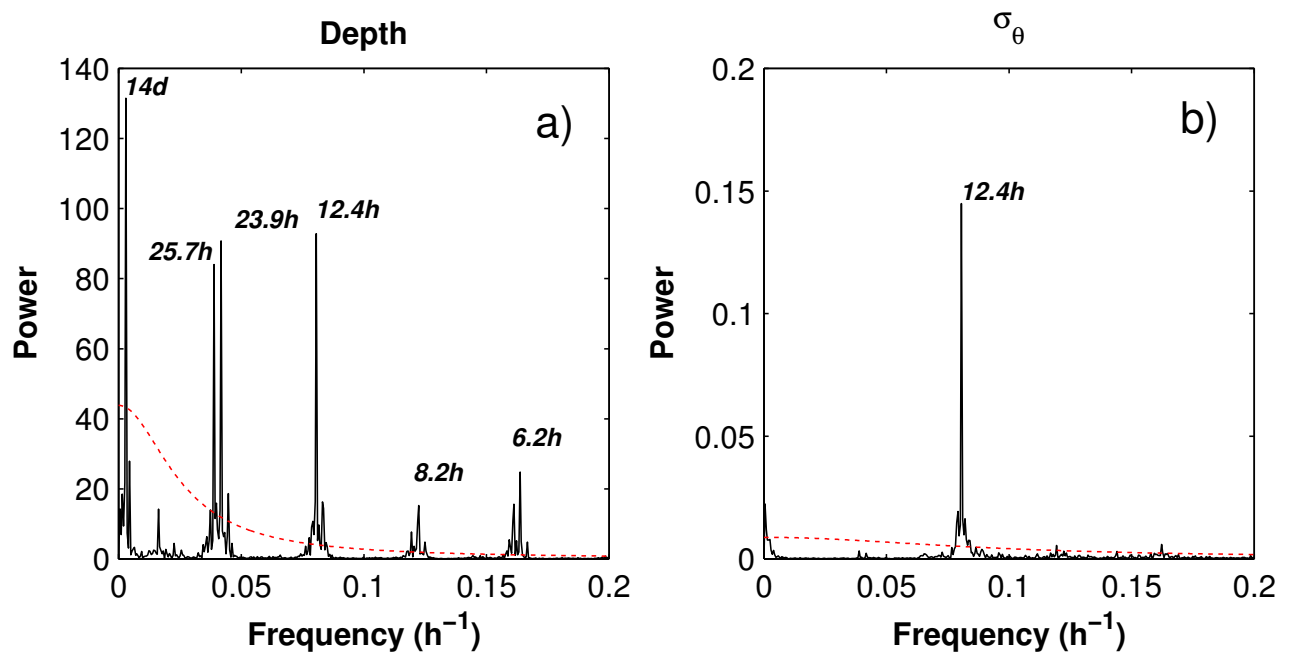


Figure 5.

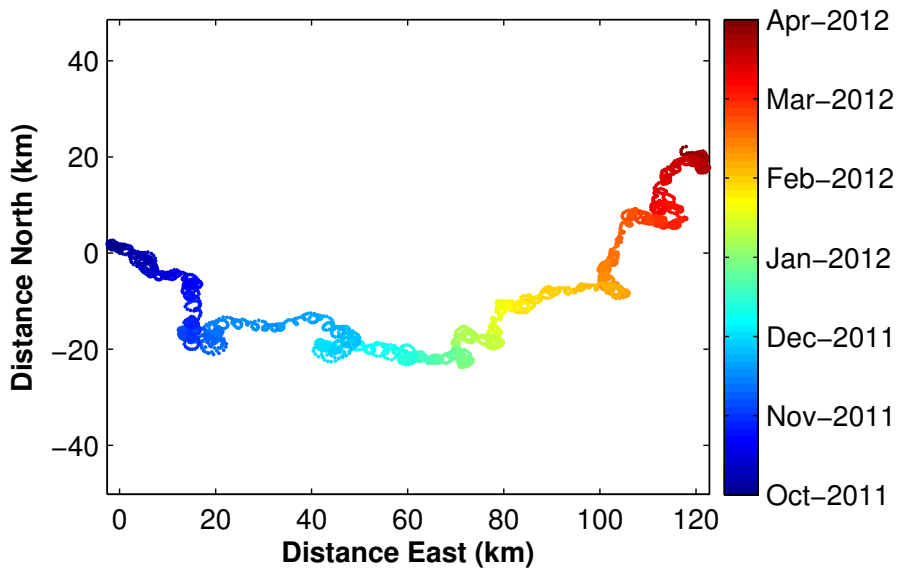


Figure 6.

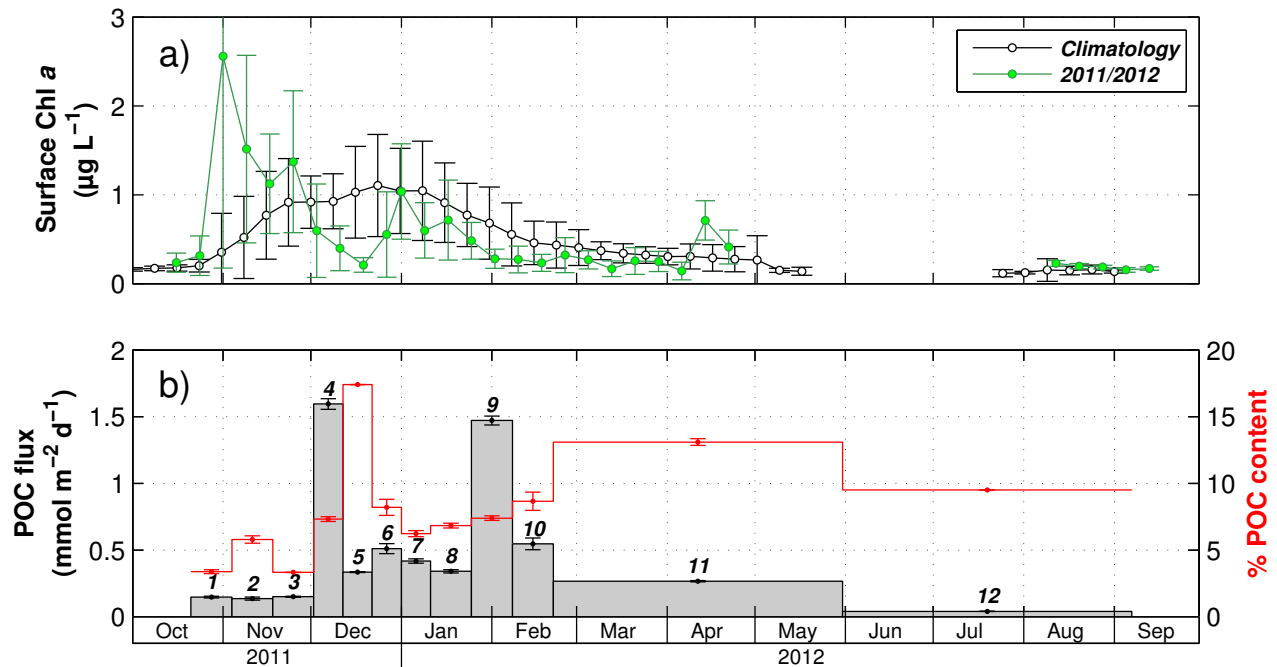


Figure 7.